Gulf General Atomic
Incorporated

AEC RESEARCH AND DEVELOPMENT REPORT

GA-8634

DIAGNOSTIC AND THERMOMETRY METHODS FOR IN-PILE THERMIONIC CONVERTER TESTING

M. K. Yates and J. W. Holland

Prepared under
Contract AT(04-3)-167
Project Agreement No. 14
for the
San Francisco Operations Office
U. S. Atomic Energy Commission

January 1, 1969

DISCLAIMER

Gulf General Atomic
Incorporated
P.O. Box 608, San Diego, California 92112

AEC RESEARCH AND
DEVELOPMENT REPORT

GA-8634
C-93b, Advanced Concepts for Future
Application - Conversion Devices
M-3679

DIAGNOSTIC AND THERMOMETRY METHODS FOR IN-PILE THERMIONIC CONVERTER TESTING

M. K. Yates and J. W. Holland

Prepared under
Contract AT(04-3)-167
Project Agreement No. 14
for the
San Francisco Operations Office
U. S. Atomic Energy Commission

Project 278

January 1, 1969

DIAGNOSTIC AND THERMOMETRY METHODS FOR IN-PILE THERMIONIC CONVERTER TESTING

M. K. Yates and J. W. Holland

INTRODUCTION:

This report describes the diagnostic and thermometry methods used for in-pile thermionic converters tested at Gulf General Atomic. The first section deals with the type of instrumentation used on each converter. The second section deals with the test procedure. The third section describes the data analysis which is performed and includes discussion of methods used to calculate the emitter temperature and diode input power. In addition, the calculation and interpretation of the relative power and relative efficiency are discussed in this section. Finally, a section on the errors inherent in the data and in the analysis is included.

INSTRUMENTATION:

A diagram of a thermionic converter and the test arrangement in the pool reactor are shown in Figures 1 and 2. The instrumentation on the converters consists of thermocouples, heaters, and voltage probes. The leads are brought up out of the core to the bridge where junctions are made to cables leading from the reactor room to consoles in the operating gallery. These consoles contain the recorders, heater power supplies, and controllers needed to monitor the converter operation. Data is recorded continuously on various chart recorders and periodically recorded on data sheets by the reactor operators. Data is taken by the operators every two hours at the beginning of operation of a new converter and every four hours after the first 50-100 hours of operation.

CONVERTER INSTRUMENTATION:

The converters are well instrumented with thermocouples to determine temperature profiles of the envelopes. Figure 3 shows the locations

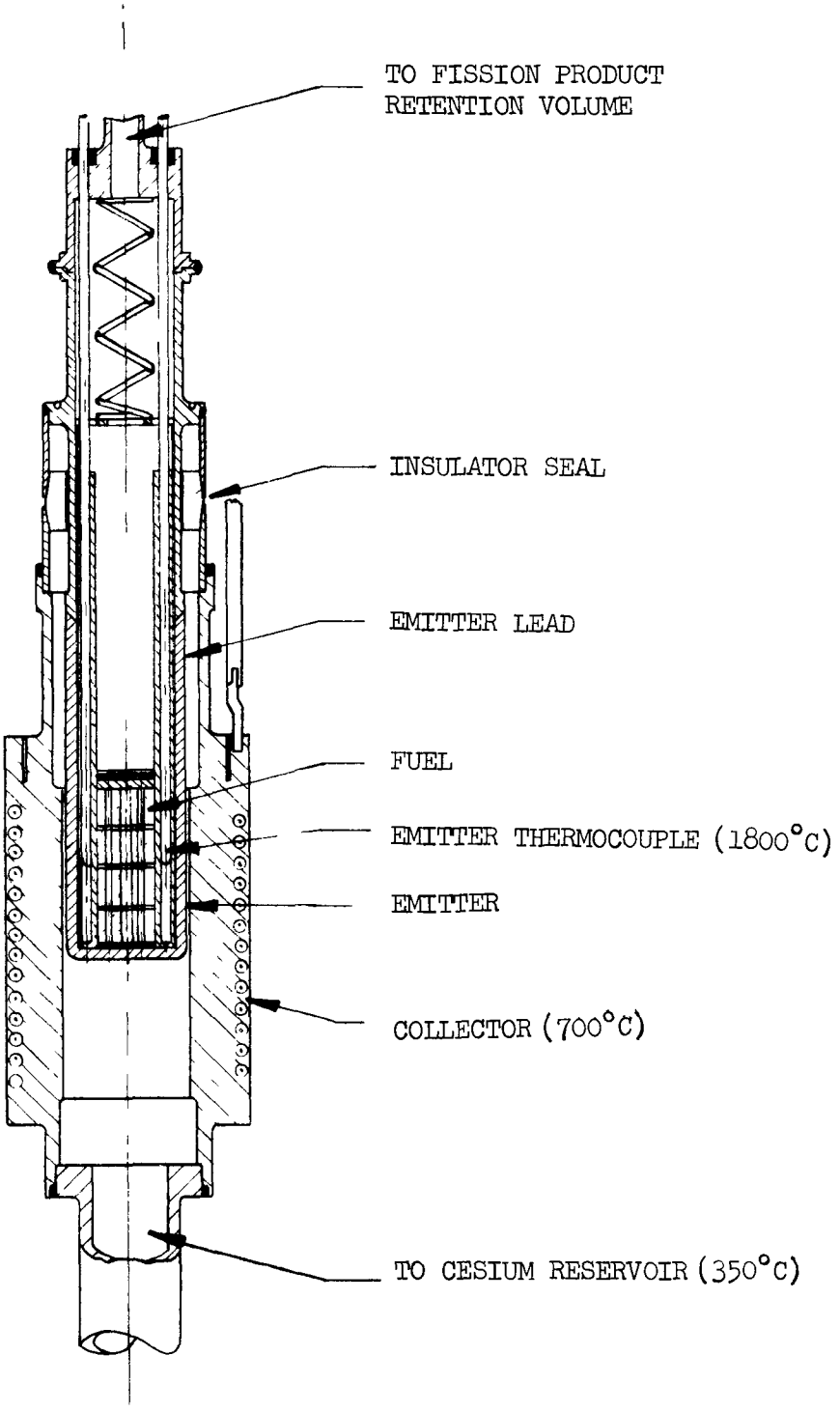

Fig. 1--Mark VI Thermionic Converter

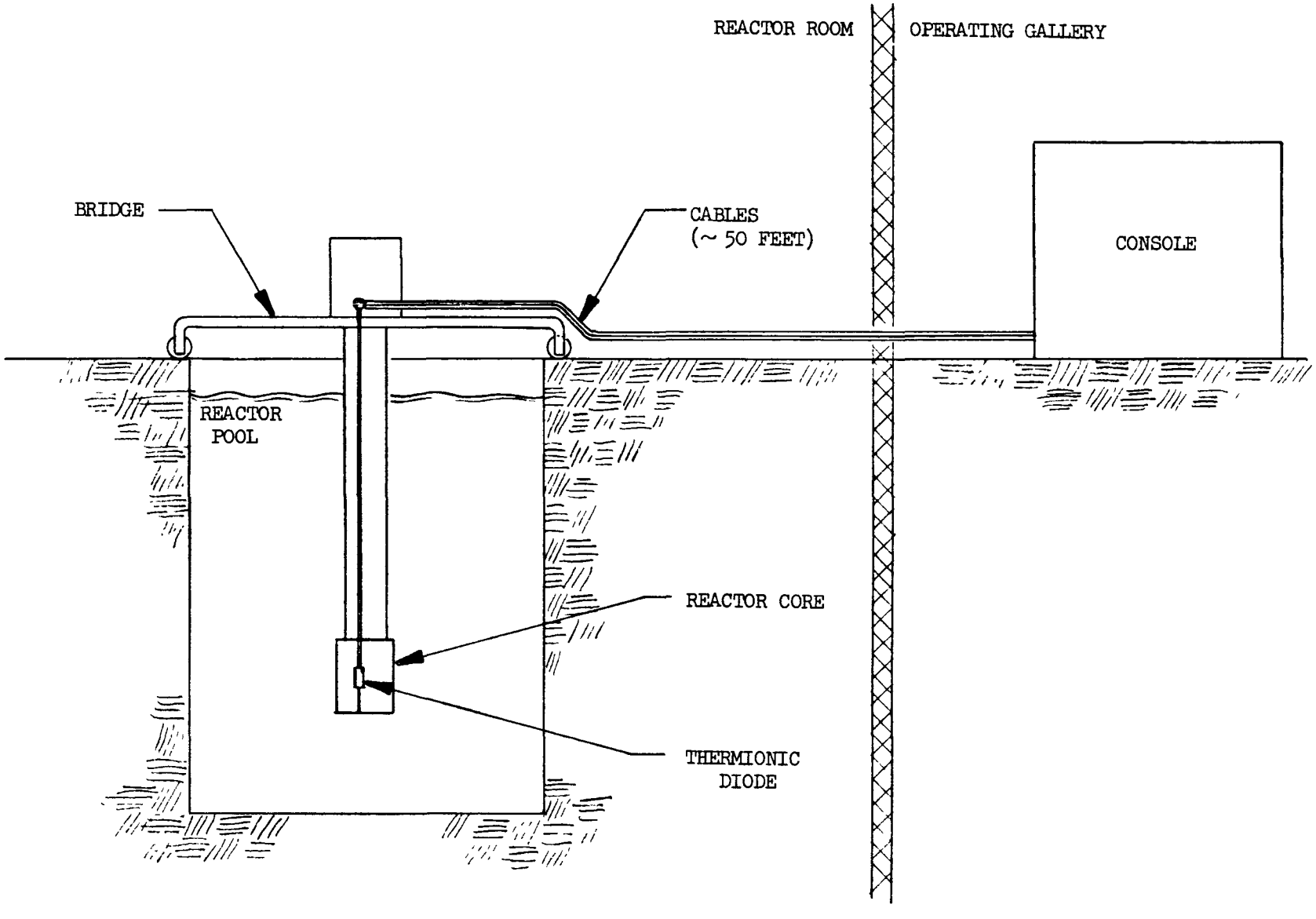

Fig. 2--Schematic diagram of pool reactor
and operating console

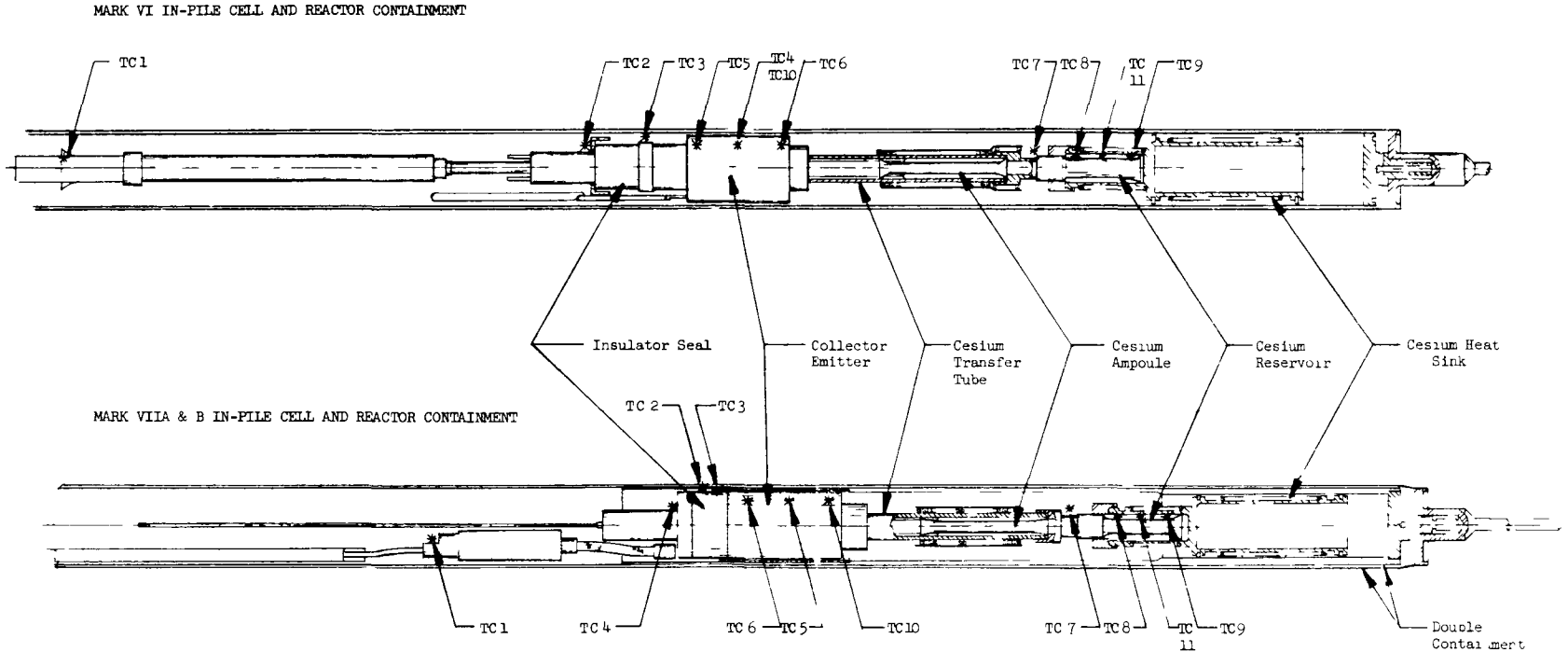

Fig. 3--Reactor Containments

of these envelope thermocouples in encapsulated Mark VI and Mark VIIA and B series converters. Usually 11 thermocouples are used:

1 on the emitter bus bar, usually near where the water cooling line is attached.

1 on the upper skirt of the converter insulator seal.

1 on the lower skirt of the converter insulator seal or on the final braze joint just below this skirt.

4 in the collector structure (one of these thermocouples is occasionally placed on the emitter cap).

1 on the cesium transfer tube just above the cesium reservoir.

3 on the cesium reservoir proper.

Floating junction, Inconel sheathed M_gO insulated chromel/alumel thermocouples are used in all of the cells. Most of the cells have used thermocouples which have a 0.040" diameter Inconel sheath; some of the later cells, particularly the Mark VIIB series have used 0.025" diameter sheaths. All of these thermocouples are aged at 1000°C for 3-4 hours, at which time their emf is checked against a standard thermocouple.

In most tests, thermocouples either in the emitter wall or in the fuel cavity are used to follow the temperature of the emitter. Current practice involves using W-5% Re/W-26% Re, BeO insulated thermocouples which are manufactured at Gulf General Atomic. The present thermocouple design is shown in Fig. 4. Generally two thermocouples are used in each converter, although four have been used on occasion. Manufacturers' tables are used for the temperature - emf relationship. A calibration check is performed on the first few thermocouples manufactured from a new batch of wire. These calibrations have almost always agreed with the manufacturers' tables within experimental errors which are estimated to be ±25°C.

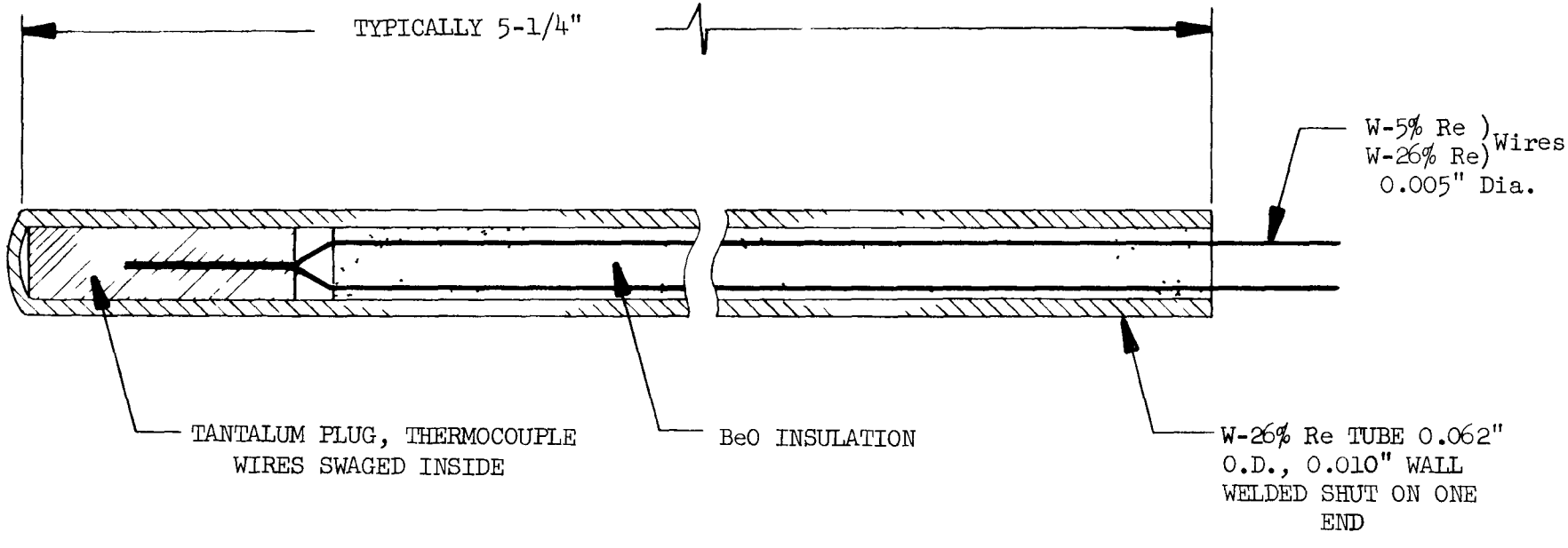

Fig. 4--W-5% Re/W-26% Re Thermocouple

Sheathed heaters are used on the cesium reservoir, cesium reservoir heat sink, cesium transfer tube, and collector (see Fig. 3). The three heaters in the cesium reservoir area provide redundancy as well as maintain the cesium temperature and ensure that the tube connecting the reservoir to the collector remains above the liquid cesium temperature. The collector heater (not provided on Mark VIIB cells) controls the collector temperature at its optimum value and keeps the emitter temperature above the vapor deposited tungsten brittle-ductile transition during shutdowns.

Voltage probes are attached to both the emitter lead and collector. These probes are usually of the same material as the cell component to which they are attached to in order to reduce thermal emfs. Also, legs of the thermocouples in the emitter or fuel cavity are used as emitter voltage probes.

A list of the converters tested along with a more detailed description of the instrumentation used on each one is given in Appendix A.

CONVERTER CONSOLES:

Operating variables measured during the tests are the cell current, lead voltage, emitter or intrafuel-clad temperature, collector temperature, cesium reservoir temperature, insulator temperature, other converter body temperatures, and heater input powers. All of the envelope temperatures except one on the cesium reservoir are recorded on a 10 position, multi-point chart recorder. The other cesium reservoir thermocouple is connected to a temperature controller which regulates the power input to the reservoir heater.

The cell current measurement is taken from a shunt. A D.C. power supply with 4% ripple is used to buck out the resistive losses in the collector and emitter bus bars. Fine adjustment of the cell current is made with a variable resistor (graphite pile). Cell current, cell voltage, and emitter (or intrafuel-clad) temperatures are recorded continuously. Heater input power levels are not recorded but are logged periodically by the reactor operators.

A diagram of the instrumentation circuits appears in Fig. 5. The variables which are used to give alarms or to scram the reactor are also shown. Alarms may be tripped by low converter current, high body temperature, or low or high pressure in the secondary containment. Scrams are activated by low current, high body temperature, or low water flow in the bus bars.

TEST PROCEDURE:

After the converter has been encapsulated in its double containment it is installed in the reactor core. Pre-operational tests which are performed prior to the installation in the core are:

1. The interelectrode spacing is examined by x-ray or gamma radiography. In addition, the cesium ampoule is examined to determine whether or not it has been opened, and the position of the fuel and fuel holddown plates are checked.
2. The resistances of the emitter, collector, sheath insulator, and inner containment tube to each other are checked to insure that no shorts exist that could prevent the operation of the converter.
3. All voltage probes, heaters and thermocouples are checked for continuity.

A plan view of the TRIGA Mark III core is shown in Fig. 6. The thermionic converters are normally positioned in the C ring (the third ring of fuel elements from the center), although they have also been operated in the D ring. Details of the TRIGA core design and operating parameters may be found in References 1 and 2. However, typical neutron and gamma fluxes in the B through E rings are listed in Table 1 at a reactor power of 1.5 Mw.

TABLE 1

Typical Neutron and Gamma Fluxes at 1.5 Mw (TRIGA Mark III)

	Neutrons, nv		Gammas
Location	Fast > 10 kev	Thermal < 0.4 eV	rads/sec
B ring	3.3×10^{13}	4.4×10^{13}	9.9×10^{4}
C	3.2	3.5	8.3
D	3.0	3.0	6.6
E	2.7	2.7	5.0

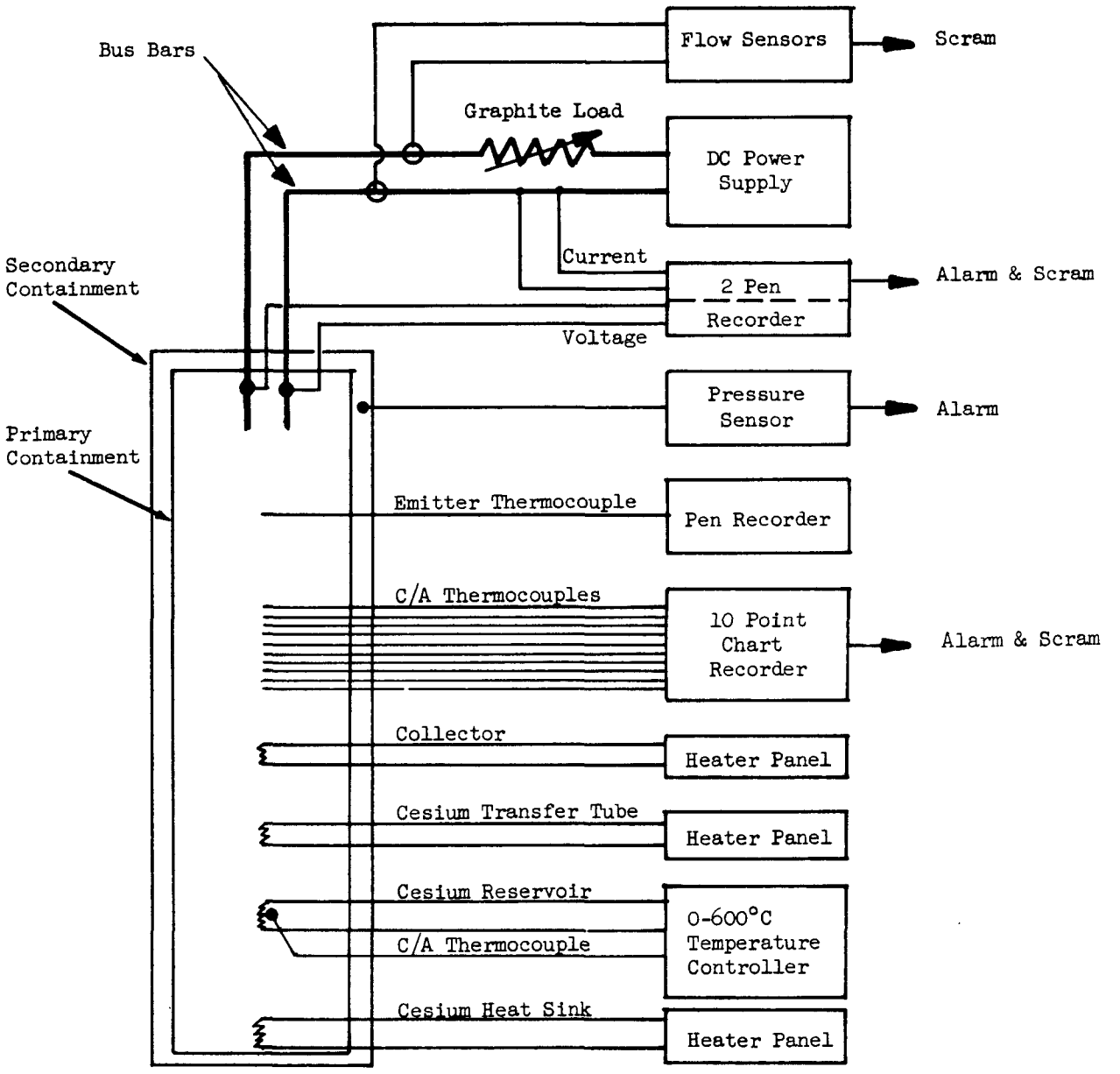

Fig. 5--Converter Instrumentation

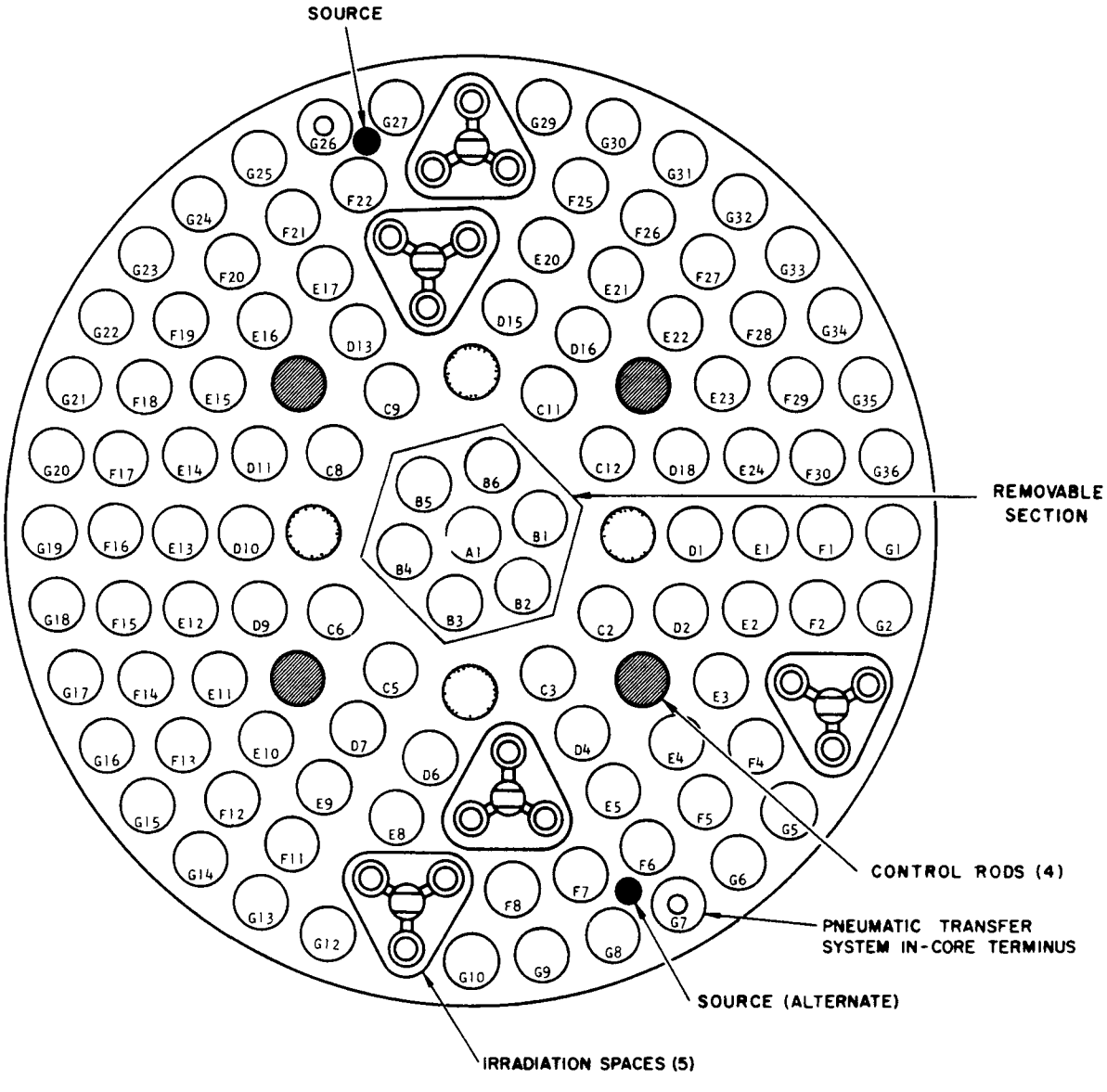

Fig. 6--Plan view of core arrangement - TRIGA Mark III

Gamma heating rates have been calculated to be 0.25-0.30 watts/gram Mw in the C ring in the molybdenum collectors of our thermionic converters.(3)

The thermionic converters are normally operated with the center of the emitter at the midplane of the reactor core. However, they can also be operated up to five inches above this point. The converters are held in place by clamping on the containment can at the reactor bridge. They are raised or lowered manually.

After all converters have been installed in the core and the core excess checked, the reactor is started up in power. The emitter (or fuel) temperature of the converter is used to monitor startup. This temperature is usually increased from 20°C-1700°C in about 45 minutes on a steady rate of increase. When the emitter temperature reaches ~ 1700°C the temperature of the cesium reservoir is brought up to provide a cesium pressure of approximately 10 torr (366°C). At these conditions the converter will produce power and the current density is gradually increased up to the usual level of 10 amps/cm^2. This last operation generally takes approximately 15 minutes and involves raising the current and reactor power together in order to hold a constant emitter temperature. Once the converter is at the desired operating conditions cesium pressure optimizations are performed and other diagnostic data is taken if desired.

This startup procedure is typically used both at the beginning of life of a converter and after a scheduled shutdown. However, after a scram the reactor is usually brought back to power at a uniform rate over a period of about 45 minutes. Since all converter power supplies are left on the converter will come back to the pre-scram conditions when the reactor is returned to the original power level.

During steady state operation of the converters the reactor power is controlled by the use of calibrated ion chambers placed outside the core. Operation continues until the failure of a converter or the depletion of the fuel. Reactor cycles last ~ 600-700 hours when four control rods are used. Recently a fifth control rod was added which has provided continuous operation for 1200 hours.

DATA ANALYSIS:

The data recorded by the reactor operators is punched on IBM cards for processing by a data analysis program. Some of the quantities that are calculated are the lead and electrode power density, emitter temperature, relative power, power input, and relative efficiency. The calculation of the last four quantities will be described in detail.

EMITTER TEMPERATURE CALCULATION:

Although thermocouples have been placed in the fuel cavity in some tests, their indicated temperature has not been used as the emitter surface temperature. They have been used only as indicators of this temperature. There are several reasons for this: First, the thermocouples have usually been in thermocouple wells which have not been in metallurgical contact with the emitter clad. Because of this, the temperature indicated by the thermocouple is effected by the degree of contact between emitter clad, fuel, and thermocouple well; also the thermocouples are usually placed in an axial position where they will tend to indicate the maximum temperature. The average surface temperature may be 50-100°C less than this value depending upon cell geometry; finally, degradation of thermocouple emf has been suspected in several tests.

For these reasons, the initial emitter temperature is set by a normalization procedure which is described below. Changes in emitter temperature are computed by means of a correlation that relates changes in cell voltage to differences in plasma losses arising from cesium pressure changes required to maintain maximum cell voltage. The details of this correlation are given in Appendix B (GA-7298).

Changes in the optimum cesium reservoir temperature during cell operation can be caused by changes in the operating parameters, current density or emitter temperature (the collector temperature is assumed to have a negligible effect on the cesium reservoir temperature). Also changes in optimum cesium reservoir temperature can be caused by

alteration of the electrode work functions which require different optimum cesium pressures to provide the necessary cesium coverage on the electrode surface. These changes in cesium pressure have been shown[4] to change the plasma loss of the converter, V_d. Considering these three variables we can write a difference equation for the change in optimum cesium reservoir temperature as follows:

$$\Delta T_r = \frac{\partial T_r}{\partial T_e} \cdot \Delta T_e + \frac{\partial T_r}{\partial J} \cdot \Delta J + \frac{\partial T_r}{\partial V_d} \cdot \Delta V_d \qquad (1)$$

T_r = Optimum cesium reservoir temperature

T_e = Emitter Temperature

J = Current Density

V_d = Plasma Loss

Where the differences, ΔX, are defined by (for all except ΔV_d)

$\Delta X = X_t - X_o$

= the value at time t minus the value at the chosen initial conditions, o.

Now the difference in plasma loss, ΔV_d, is equal to the calculated electrode voltage at time t, V_t, less the initial voltage evaluated at the same emitter and collector temperatures and current density of time t, V_{ot}. Therefore,

$$\Delta V_d = V_t - V_{ot} \qquad (2)$$

Using a linear fit for a thermionic equation (Appendix B) which relates electrode voltage, emitter temperature, collector temperature, and current density at the optimum cesium reservoir temperature, we have:

$$V_{ot} = a(J_t)\ T_{et} - b(J_t) - \delta b(T_{ct}) \qquad (3)$$

T_{ct} = Collector temperature at time t

$a(J_t)$ and $b(J_t)$ are used to fit equation(3) to measured data

δb = A correction to the cell voltage which depends upon how far off optimum the collector temperature is.

Again, from Appendix B:

$$\delta b = 4.14 \times 10^{-6} (T_c - T_{c\ opt})^2 \text{ volts} \qquad (4)$$

Where

$T_{c\ opt}$ = Optimum collector temperature (measured during performance mapping or set by comparison to other cells).

Plots of equations (3) and (4) for a Mark VI out-of-pile W/Mo cell (OC-5) are shown in Figures 7 and 8.

Now by adding and subtracting a $(J_t)\ Te_o$ to equation (3) we can transform it to:

$$V_{ot} = a(J_t)\ \Delta T_e - b(J_t) - \delta b(T_{ct}) + a(J_t)\ Te_o \qquad (5)$$

Substituting (2) and (5) into (1) and solving for ΔT_e

$$\Delta T_e = \frac{\Delta T_r - \frac{\partial T_r}{\partial V_d}\left[V_t + b(J_t) + \delta b(T_{ct})\right] + \frac{\partial T_r}{\partial V_d} \cdot a(J_t) \cdot Te_o - \frac{\partial T_r}{\partial J} \cdot \Delta J}{\frac{\partial T_r}{\partial T_e} - \frac{\partial T_r}{\partial V_d} \cdot a(J_t)} \qquad (6)$$

Except for $\frac{\partial T_r}{\partial V_d}$ all quantities of equation (6) are either measured at time t or evaluated during the performance mapping of the converter. The quantity $\frac{\partial T_r}{\partial V_d}$ was taken from Reference 4 and is equal to -165°C/volt. The values of the measured coefficients are listed in Table 2 for all cells tested thus far.

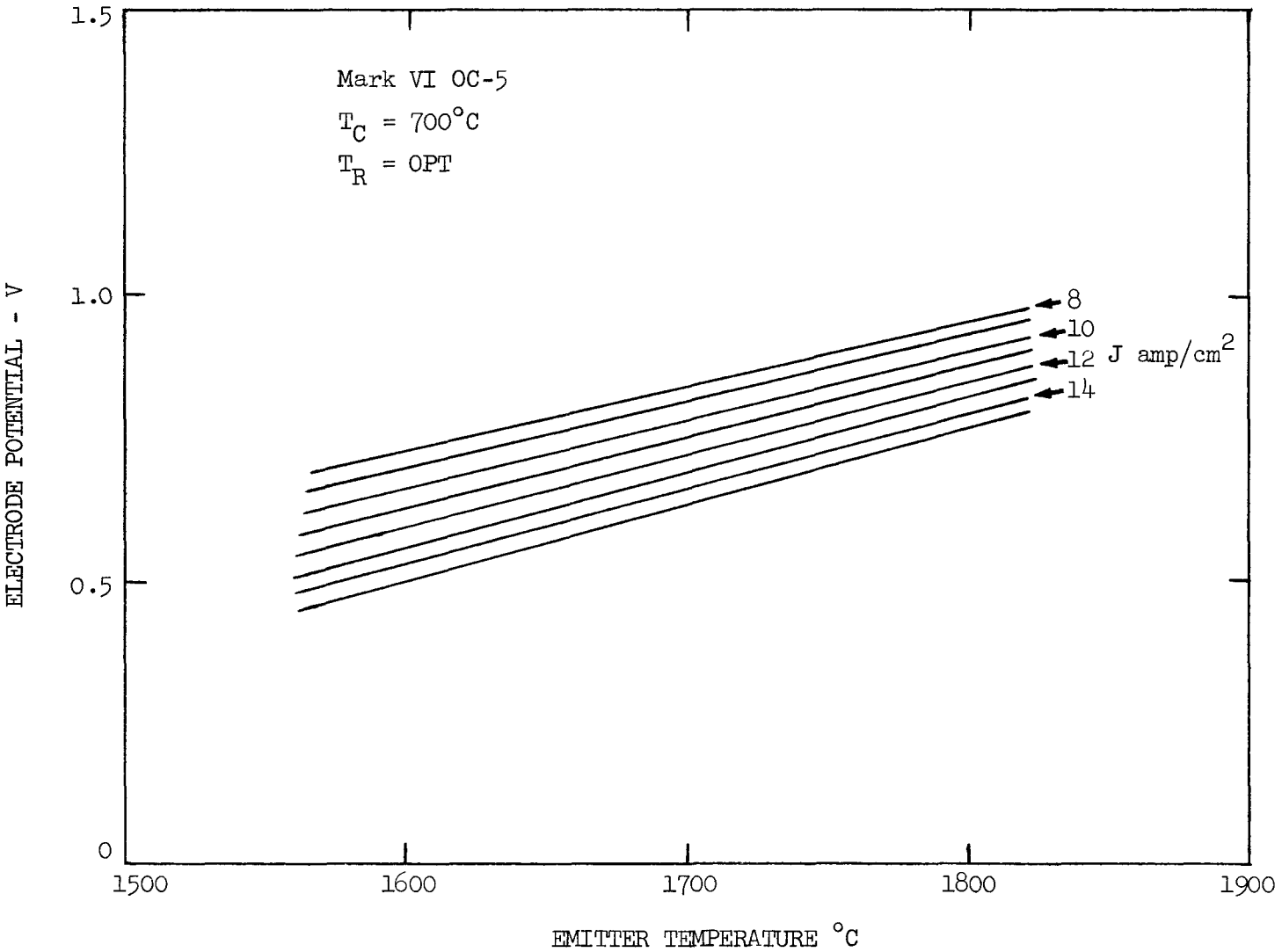

Fig. 7--Electrode potential versus emitter temperature of Mark VI OC-5

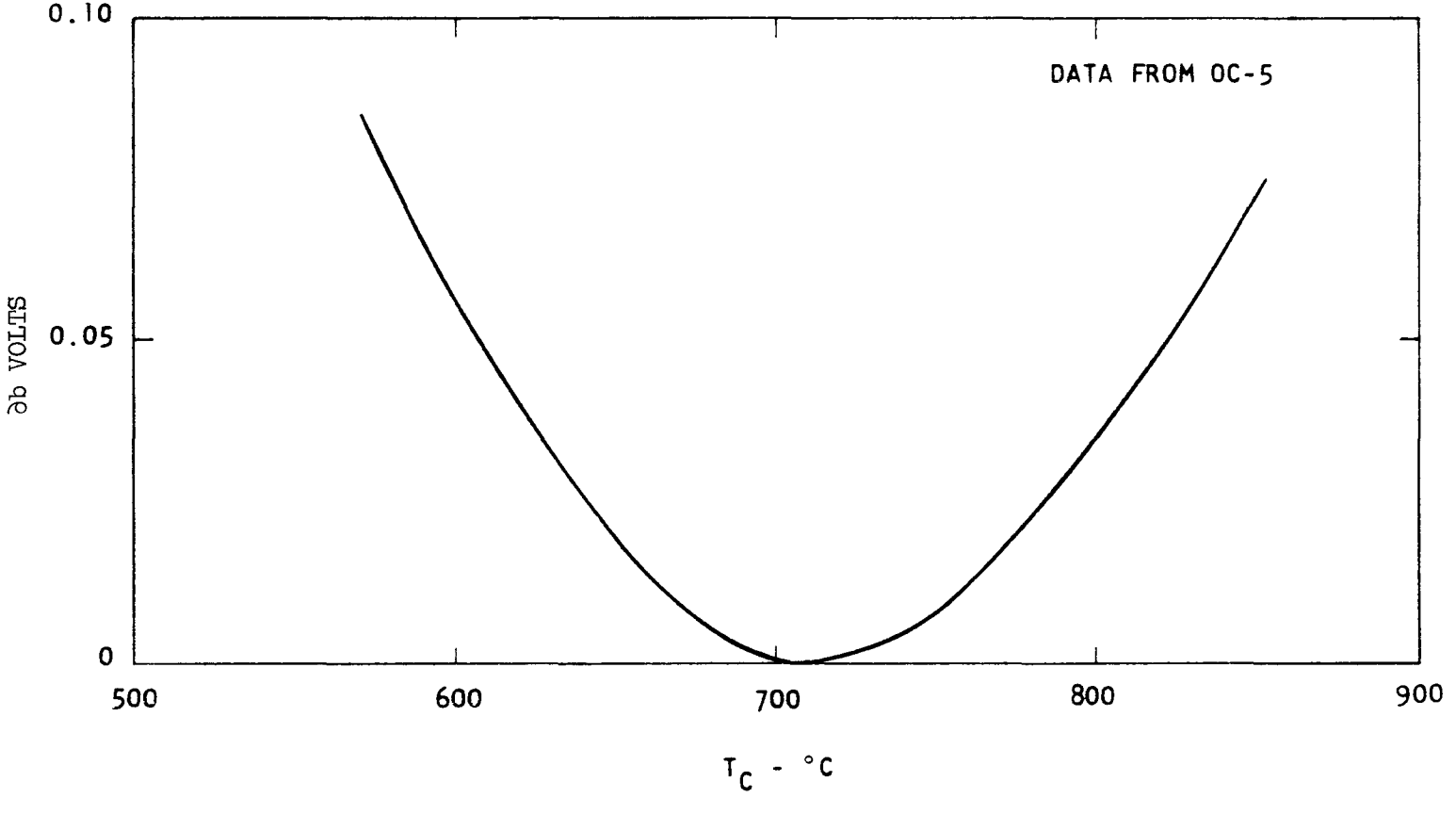

Fig. 8--Voltage correction for deviations of collector temperature from optimum

TABLE 2

Measured Coefficients and Normalization for In-Pile Cells

Quantity	IC-4 to IC-11	IC-12	IC-13	IC-14	IC-15	IC-16	FEI-1	FEI-2	FEI-3	FEI-4	FEI-5
Electrode Material Emitter/Collector	W/Mo	→				→	W/Mo	W/Mo	W/Nb	W/Nb	W/Nb
Fuel	UC-ZrC	→		→	UO_2	UC-ZrC	UC-ZrC	UC-ZrC	UO_2	UC-ZrC	UO_2
Optimum Collector Temperature °C	710.	782.	762.	783.	820.	740.			785.	750.	
Constants											
fit for "a" $a_0 \times 10^3$ volt/°C	1.163	4.78	2.65	3.11	2.8	1.992			2.289	2.067	
$a=a_0+a_1J+a_2J^2$ $a_1 \times 10^5$ volt/°C/amp/cm^2	5.168	-23.0	-19.0	-19.4	-10.0	-3.37			-8.18	-7.98	
$a_2 \times 10^7$ volt/°C/amp^2/cm^4	-37.8	-	-	-	-	-	Same as IC-4	Same as IC-4	-	-	Same as FEI-3
fit for "b" b_0 volt	0.893	6.32	2.93	3.93	3.59	2.334			2.815	2.420	
$b=b_0+b_1J+b_2J^2$ $b_1 \times 10^2$ volt/amp/cm^2	11.29	-31.4	-23.2	-25.4	-13.5	-2.57			-8.90	-9.883	
$b_2 \times 10^4$ volt/amp^2/cm^4	-61.8	-	-	-	-	-			-	-	
$\frac{\partial T_r}{\partial T_e}$ °C/°C	0.18	0.026	0.055	0.08	0.11	0.10			0.05	0.06	
$\frac{\partial T_r}{\partial J}$ °C/amp/cm^2	2.1	3.8	3.8	3.5	3.0	3.0			2.0	2.0	
Out-of-pile cell used for normalization	OC-5	→				→	OC-5	OC-5	LC-7	→	→
Percentage of power output of standard cell that was assumed	100.	100.	100.	83.	100.	81.	100.	100.	100.	121.	100.
Relative Power & Relative Efficiency normalized to unity at (S.U. = > start-up)	S.U.	S.U.	S.U.	800 hrs	161 hrs	20 hrs	S.U.	S.U.	7 hrs	27 hrs	26 hrs

NOTE: The OC-5 coefficients are those listed for IC-4 to IC-11

There are at least two types of changes which may cause errors in the calculation of the changes in emitter temperature. Changes in contact potential of the electrodes which may occur along with work function changes are not taken into account. Probably only changes in the collector work function are important here because reoptimization of the cesium pressure should keep the cesiated emitter work function at its optimum value. Also, possible voltage losses due to the presence of inert gas in the interelectrode space are not accounted for. If either of these changes occur the calculated emitter temperature will change independently of whether or not the true emitter temperature is changing.

RELATIVE POWER CALCULATION:

The relative power, P_r is defined as the fraction of the output power corrected to conditions of time, t, (except for the cesium reservoir temperature which is optimized) that can still be produced at time t. Deviations in the relative power from unity are interpreted to be caused by work function changes, alterations in the interelectrode gap or in the scattering of electrons by a foreign gas.

Again from Appendix B:

$$P_r = \frac{P_t}{P_{ot}} \tag{7}$$

Where

P_t = The cell output power at the electrodes at time t

P_{ot} = The initial output power corrected to the collector temperature, emitter temperature, and current density at time t.

Therefore

$$P_{ot} = V_{ot} \; J_t$$

$$P_t = V_t \; J_t$$

Where V_{ot} is defined in Equation (3) and therefore

$$P_r = \frac{V_t}{V_{ot}} \tag{8}$$

Limitations described above for the emitter temperature calculation apply also to the relative power calculation. If changes in contact potential or leakage of inert gas into the interelectrode space occur, the calculated emitter temperature will change in order to maintain the relative power at a constant value.

POWER INPUT CALCULATION:

The initial power input cannot be measured in-pile and is set by the normalization procedure described below. Changes in the power input are calculated using an energy balance on the collector. Those parameters used are the measured collector temperature, collector heater power, cell output power, and calculated emitter temperature. From Appendix B:

$$\Delta Q = U\Delta T_c - Q_{CH} + \frac{\partial Q_{el}}{\partial T_e} \cdot \Delta T_e + \Delta P \tag{9}$$

with

Q = the power input to the diode

U = a measured heat transfer coefficient from the collector to the reactor pool water

Q_{CH} = the collector heater power

P = the cell output power

$\frac{\partial Q_{el}}{\partial T_e}$ = the change in emitter end losses due to changes in temperature

and $\Delta X = X_t - X_o$ as previously described.

RELATIVE EFFICIENCY CALCULATION:

The relative efficiency, η_r, is defined in a manner analogous to the relative power. Deviations in the relative efficiency from unity arise from the combined effects of changes in the relative power and changes in thermal transport such as would result from an electrode emittance change or from a change in electron waste heat (electron waste heat is the sum of the kinetic energy of electrons entering the collector and the energy equivalent of the collector work function). In the fission heated converters the environment is an inert gas, either helium or argon so that inleakage of these gases would also contribute to the thermal transport if such were to occur. Inleakage of fission gas from the fuel chamber into the converter is another possibility.

$$\eta_r = \frac{\eta_t}{\eta_{ot}} \tag{10}$$

Where

$\eta_t = \frac{P_t}{Q_t}$ = the cell electrode output power divided by the total input power at time t.

$\eta_{ot} = \frac{P_{ot}}{Q_{ot}}$ = the chosen initial cell output power divided by input power corrected to the conditions at time t.

therefore

$$\eta_r = P_r \frac{Q_{ot}}{Q_t} \tag{11}$$

Where

$Q_t = Q_o + \Delta Q$ = the initial input power plus the change in input power calculated previously.

Q_{ot} has been taken from the OC-5 data. A graph of this data is shown in Fig. 9. In cells where the emitter area hasn't been the same as OC-5, Q_{ot} was scaled accordingly.

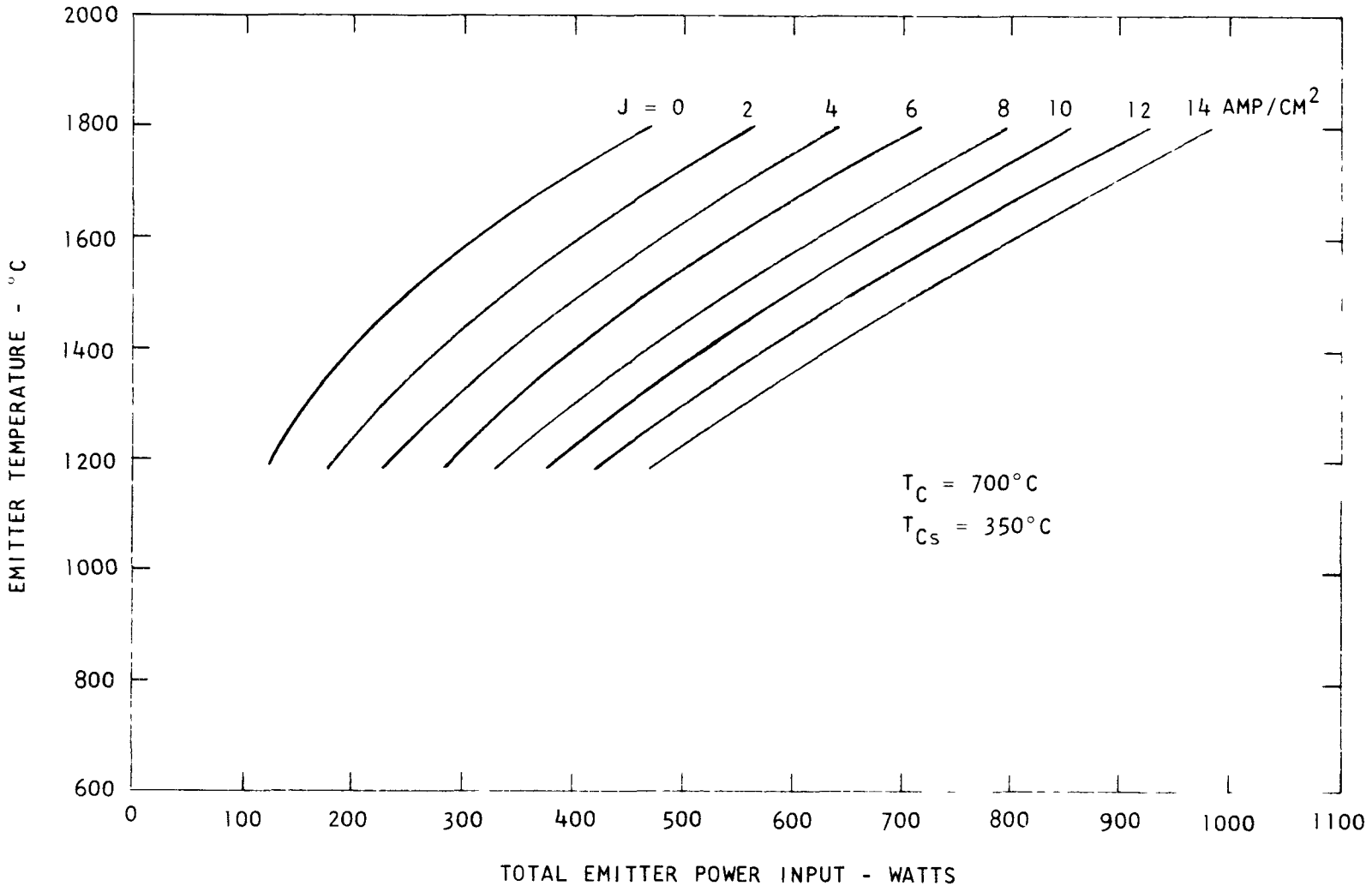

Fig. 9--Mark VI OC-5 emitter temperature versus input power with current density shown as a parameter

NORMALIZATION PROCEDURES:

As mentioned previously, two quantities are set by normalization, the initial emitter temperature, T_{eo}, and power input, Q_o. This normalization consists of comparing the measured cell current, cell voltage, and collector temperature with that of out-of-pile cells whose emitter temperatures and power inputs were accurately determined. The out-of-pile cells used for normalization, the percentage of the power output of the standard cell which the cell in question was assumed to produce, and the time at which the normalization was performed are listed for all cells tested to date in Table 2.

As shown in the table two out-of-pile cells have been used for normalization, OC-5 for W/Mo cells[5] and LC-7 for W/Nb converters.[6] The performance of OC-5 has been compared to that of other W/Mo cells. One comparison is shown in Fig. 10 where the maximum output power density is plotted against emitter temperature for OC-5 and for a TECO converter.[7] Good agreement is obtained. No similar comparisons have yet been made for LC-7.

Initial Emitter Temperature

For most cells, the initial emitter temperature was set by assuming that the cell produced the same power output (at some current density and at optimum collector and reservoir temperatures) as the standard cell. Therefore, specifying the electrode voltage and current density, Fig. 7 was used to specify the initial emitter temperature. The emitter temperature predicted in this manner was then compared with the intrafuel cladding temperature and with the saturation current density observed during emitter work function measurements. Three values of emitter temperature could be obtained:

1. T_{e_1}, the value from performance comparison.
2. T_{e_2}, the value of the intrafuel cladding temperature.
3. T_{e_3}, the value calculated from the saturation current density at a high enough T_e/T_r to obtain the emitter base work function (using a value for vapor deposited tungsten of 4.55 eV).

If these values were consistent ($T_{e_1} \gtrsim T_{e_2}$ - 100°C for carbide cells, $T_{e_1} \gtrsim T_{e_2}$ - 200°C for oxide cells, since a temperature drop is expected

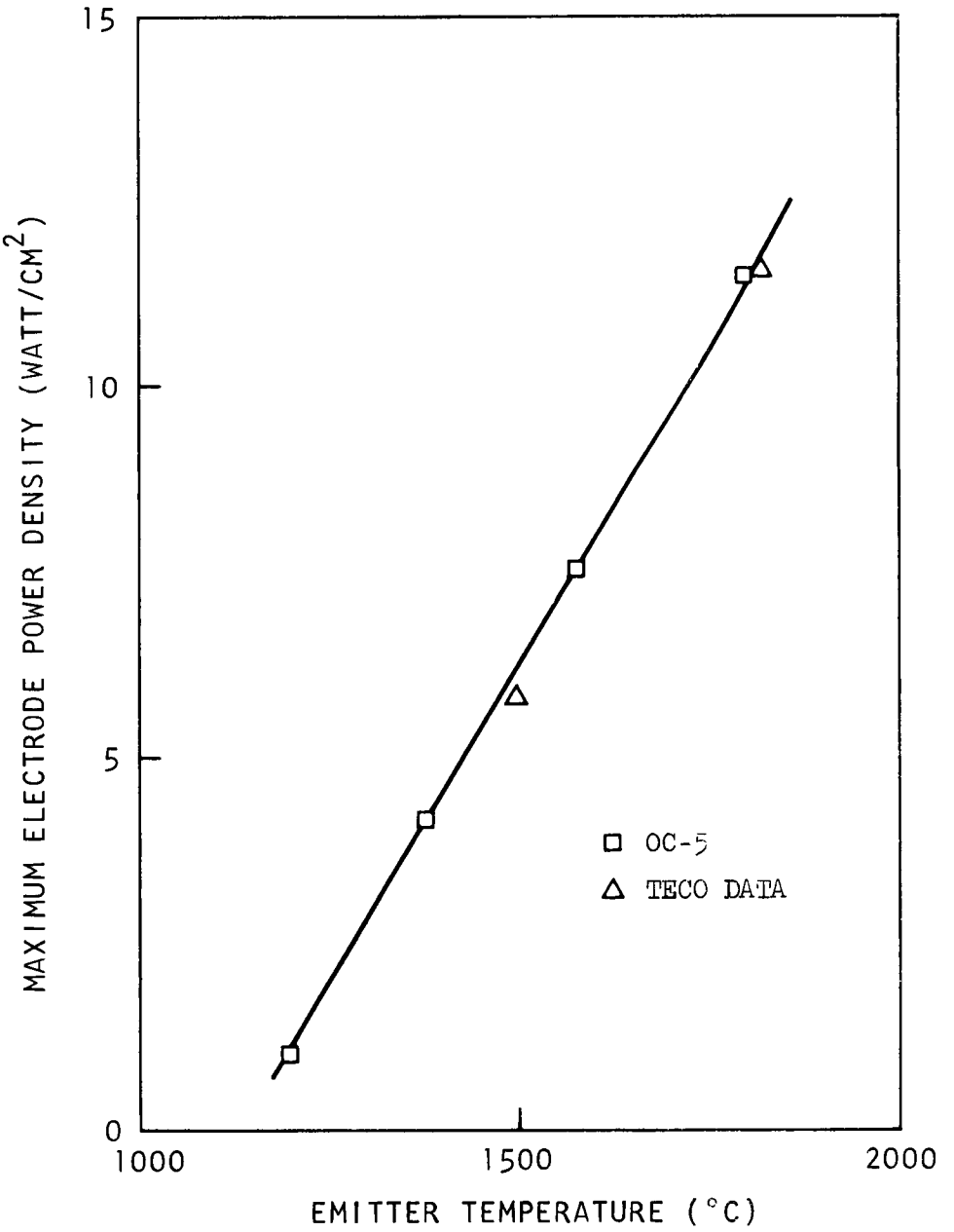

Fig. 10--Maximum electrode power densities of OC-5 as a function of emitter temperature with comparison to TECO data

between the fuel cavity and emitter surface; $T_{e_1} \simeq T_{e_3}$, since these temperatures should be the same), then T_{e_1} was used as the initial emitter temperature. However, in IC-14, IC-16, and FEI-4, these quantities were not consistent.

In IC-14 and IC-16, lower performance than OC-5 was suspected at or shortly after start-up. Therefore, in IC-14, the initial emitter temperature was set at 50°C below the initial intrafuel cladding temperature. This implied that the cell was capable of producing approximately 83% of the power output of OC-5. A similar procedure was followed in IC-16 where the emitter temperature was arbitrarily set 80°C below the intrafuel clad temperature. This normalization implied that the cell was capable of producing 81% of the power output of OC-5.

The initial output of FEI-4 appeared higher than the out-of-pile standard. The availability of detailed saturated emission data made possible a different procedure on this cell. The trade-offs between emitter bare work function (it appeared higher than 4.55 eV), voltage output, and the difference between emitter and intrafuel clad temperature were all calculated. Differences in voltage output were estimated by assuming that a 0.10 eV increase in bare work function increased the cell power output by 10%. Unique values of bare emitter work function and emitter-intrafuel clad temperature difference were then determined. A bare work function of 4.76 eV was calculated, implying a 21% performance advantage over the out-of-pile standard.

Initial Power Input

After calculating T_{eo}, the total power input was read from Fig. 9, then scaled to the cell in question by comparing its emitter area with that of OC-5.

ERROR ANALYSIS:

This section will cover the errors involved in setting the initial emitter temperature and power input as well as those inherent in the calculations of changes in both emitter temperature and power input and in the relative power and efficiency. Also the uncertainties which must be taken into account when comparing two cells will be discussed. All errors discussed will be in terms of $\pm\sigma$ (one standard deviation).

Errors in Initial Normalizations

No direct comparison of in-pile cells is possible but it is estimated that the error in the initial emitter temperature is ±50°C and that in the initial power input is ±20%.

Errors in Calculated Quantities

First, the errors inherent in the measured data and in the coefficients used in the equations were estimated (see Table 3). Then these errors were propagated using the equations given and the standard procedure for propagating independent errors:

that is, if we are given

$$F = f(x, y, z, \ldots)$$

then, if the uncertainties in x, y, z,...are given as Δx, Δy, $\Delta z, \ldots$, the error in F is ΔF and

$$\Delta F = \pm \left[\left(\frac{\partial F}{\partial x} \Delta x \right)^2 + \left(\frac{\partial F}{\partial y} \Delta y \right)^2 + \frac{\partial F}{\partial z} \Delta z)^2 + \ldots \right]^{\frac{1}{2}} \qquad (12)$$

For the purposes of these calculations the dependence of the four calculated quantities, changes in emitter temperature, ΔT_e, changes in power input, ΔQ, relative power, P_r, and relative efficiency, η_r, were assumed to be:

$$\Delta T_e = f\left(T_r, V, J, \frac{\partial T_r}{\partial V_d}, \frac{\partial T_r}{\partial J}, \frac{\partial T_r}{\partial T_e}\right)$$

$$\Delta Q = f\left(T_c, \Delta T_e, Q_{CH}, U, \frac{\partial Q_{el}}{\partial T_e}\right.$$

$$P_r = f(V, \Delta T_e, J)$$

$$\eta_r = f(V, \Delta T_e, J, \Delta Q)$$

Using these forms for the dependency, partial derivatives were calculated and the errors in the quantities were calculated.

Table 3

Accuracy of Measured Data and Coefficients

Quantity	$\pm\sigma$
Quantities measured during test	
Cell voltage, V	±0.02V
Cell Current Density, J	± 2 amp/ emitter area
Collector Temperature, T_c	±5°C*
Cesium Reservoir Temp, T_r	±5°C*
Collector Heater Power, Q_{CH}	±3%
Quantities measured during performance mapping	
Collector/Pool Water Heat Transfer Coefficient, U	±30%
$\frac{\partial T_r}{\partial J}$	±50%
$\frac{\partial T_r}{\partial T_e}$	±30%
$\frac{\partial T_r}{\partial V_d}$	±30%
$\frac{\partial Q_{el}}{\partial T_e}$	±30%

Using the data given in Table 3, sample calculations were performed on IC-12 at 3295 hours, and IC-15 at 2000 and at 5002 hours. The results of these calculations are given in Table 4.

Table 4

Results of Sample Error Calculations

Cell	Hours	ΔT_e °C	ΔQ watts	P_r	η_r
IC-12	3295	-69±19	318±64	0.82±0.06	0.56±0.08
IC-15	2000	+88±25	122±31	1.00±0.06	0.96±0.05
IC-15	5002	+71±28	151±34	1.11±0.07	1.01±0.06

*does not include errors related to axial or radial temperature gradients

Table 5 lists the breakdown of the sources of error for the four calculated quantities. As shown in the table, the most important contributors of error for each quantity are:

ΔT_e: T_r, V
ΔQ: T_c, Q_{CH}, U
P_r: ΔT_e, V
η_r: ΔT_e, ΔQ, V

Errors to be Considered When Comparing Converters

When comparing the measured data from two converters, the accuracy of some of the quantities previously listed may have to be adjusted. The accuracy listed for the initial emitter temperature ±50°C, and initial power input, ±20%, are the expected accuracy for comparison of converters. Also, the errors in cell voltage, current density, and collector heater power (as listed in Table 2) of different converters should be equivalent. However, an allowance for temperature distributions must be made for collector and cesium reservoir temperatures. In the collector temperature, the possibility of radial temperature gradients requires the error assumed for converter comparison to be ±25°C. An absolute accuracy of the cesium reservoir temperature of ±15°C is based on the existance of an axial temperature distribution, which has been as large as 50°C/inch in the reservoir area, and the uncertainty of the location of the liquid level.

TABLE 5

Sources of Error for 4 Calculated Quantities

				Error in Quantity due to Assumed Error in Variable											
	Cell	Hours	Total Error	V	J	T_c	T_r	Q_{CH}	U	$\frac{\partial T_r}{\partial J}$	$\frac{\partial T_r}{\partial T_e}$	$\frac{\partial T_r}{\partial V_d}$	$\frac{\partial Q_{el}}{\partial T_e}$	ΔT_e	ΔQ
ΔT_e	IC-12	3295	±19°	±8	±8	--	±13	---	---	±8	±4	±3	---	---	--
	IC-15	2000	±25°	±13	±2	--	±20	---	---	0	±7	±2	---	---	--
	IC-15	5002	±28°	±13	±2	--	±20	---	---	0	±6	±14	---	---	--
ΔQ	IC-12	3295	±64w	--	--	±18	--	±2	±61	---	---	---	±2	±2	--
	IC-15	2000	±31w	--	--	±23	--	±15	±13	---	---	---	±2	±2	--
	IC-15	5002	±34w	--	--	±23	--	±16	±13	---	---	---	±2	±2	--
P_r	IC-12	3295	±.06	±.03	±.02	--	--	---	---	---	---	---	---	±.04	--
	IC-15	2000	±.06	±.04	±.01	--	--	---	---	---	---	---	---	±.05	--
	IC-15	5002	±.07	±.04	±.01	--	--	---	---	---	---	---	---	±.06	--
η_r	IC-12	3295	±.08	±.02	±.01	--	--	---	---	---	---	---	---	±.07	±.03
	IC-15	2000	±.05	±.03	±.01	--	--	---	---	---	---	---	---	±.02	±.03
	IC-15	5002	±.06	±.03	±.01	--	--	---	---	---	---	---	---	±.03	±.03

REFERENCES

1. Mikesell, R. E., "TRIGA Experimental and Irradiation Facilities for Research and Development," General Dynamics, General Atomic Division Report GA-1695, Rev. 5, November 1966.

2. West, G. B., "Calculated Fluxes and Cross Sections for TRIGA Reactors," General Dynamics, General Atomic Division Report GA-4361 and Supplements A & B, August 1963.

3. Hackney, R., (Gulf General Atomic) Private Communication.

4. Kitrilakis, S. S., et al., "The Department of the Observed Performance from the Idealized Case in Cesium Thermionic Converters," in Report on Twenty-Fourth Annual Conference on Physical Electronics, March 1964, Massachusetts Institute of Technology, Cambridge, Massachusetts, p171-184.

5. Holland, J. W., "Performance and Energy Transfer Measurements on Cylindrical Cesium Thermionic Converters," General Dynamics, General Atomic Division Report GA-4729, November 1963.

6. Holland, J. W., and J. Kay, "Performance of a Cylindrical Geometry Thermionic Converter with an Improved Work Function Tungsten Emitter," National Aeronautics and Space Administration Report GA-8172, Gulf General Atomic, Inc., June 1968.

7. Rasor, N. S., and S. S. Kitrilakis, "Basic and Engineering Implications of Correlated Converter Phenomenology," Thermionic Conversion Specialist Conference, Cleveland, Ohio, October 1964, p227.

APPENDIX A

APPENDIX A
METHODS AND ACCURACY OF DETERMINING OPERATING PARAMETERS*

	IC-4	IC-5	IC-6	IC-7	IC-8	IC-9	IC-10	IC-11	IC-12	IC-13	IC-14	IC-15	IC-16		FEI-1	FEI-2	FEI-3	FEI-4	FEI-5
A. Input power	1	1	1	1	1	1	1	1	1	1	1	1	1		1	1	1	1	1
B. Intrafuel-clad Temperature	14	14	14	14	14	14	14	14	2	2	2	3	2		2	2	2	2	2
C. Emitter Temperature	4	5	5	5	5	5	5	5	6	6	6	6	6		7	8	6	6	6
D. Collector Temperature	9	9	9	9	9	9	9	9	9	9	9	9	20		9	9	21	21	21
E. Ceramic-to-metal seal/ insulator temperature	10	10	10	10	10	10	10	10	10	10	10	10	10		10	10	10	22	22
F. Cesium pressure	11	11	11	11	11	11	11	11	11	11	11	11	11		11	11	11	11	11
G. Output: current, electrode voltage, lead voltage	12	12	12	12	12	12	12	12	13	13	13	13	13		13	13	13	13	13
H. Other diagnostic determinations	-	-	-	-	-	-	-	-	15	15	15	15	15		15	15	15	15	-
I. Type and quality of test environment	16	17	17	17	17	18	17	18	18	19	19	18	19		18	19	18	18	18

* Numbers refer to listing on following pages

KEY TO THE TABLE

1. Not measured, absolute value deduced from similar out-of-pile cells, changes calculated by the correlation described.

2. Two W-W/Re thermocouples were located in thermocouple wells within the fuel cavity and next to the inside wall of the emitter. These wells were not metallurgically bonded to the fuel cladding but were in mechanical contact. The axial location of the thermocouples from the emitter end was 1/3 of the emitter length. Calibration experiments have shown that the thermocouples at that location read approximately the maximum temperature of the axial profile. The accuracy of the calibrated thermocouples at the beginning of life was estimated to be ±25°C.

3. Four W-W/Re thermocouples were located in thermocouple wells within the fuel cavity and next to the inside wall of the emitter. These wells were not metallurgically bonded to the fuel cladding but were in mechanical contact. These four thermocouples were positioned so as to indicate the axial profile of the intrafuel-clad region. The accuracy of the calibrated thermocouples was estimated to be ±25°C.

4. Values were measured by means of four calibrated W-W/Re thermocouples located within the emitter wall at four axial locations. Their accuracy at the beginning of life was estimated to be ±25°C. In emitter temperature profile experiments it was shown that the average of the four thermocouple readings matched the average surface temperature within 25°C.

5. Not measured. Initial values were estimated according to the method described in GA-6892. Temperatures relative to the initial value were calculated by means of the method described in this report.

6. Not measured. Initial values were estimated by considering the thermionic performance, indicated work functions, and the measured intrafuel-clad temperature as described in the body of this report. Temperatures relative to the initial value were calculated by means of the method described in this report.

7. Not estimated.

8. Average emitter surface temperature was estimated by assuming a constant 100°C difference between the intrafuel-clad and surface temperatures.

9. Four inconel sheathed chromel-alumel thermocouples with isolated junctions were located within the collector structure to obtain data on the temperature distribution of the collector. Average collector temperature accuracy over the life of the converter was not estimated.

10. Two thermocouples were located on the upper and lower skirts of the ceramic-to-metal seal. They were mechanically contacted with the skirts and were estimated to correspond to the skirt temperatures within -15 to -25°C.

11. The cesium pressure was not directly measured or reported. Instead the temperature of the cesium reservoir was reported. In these in-pile converters a temperature gradient existed over the length of the reservoir. The temperature profile of the reservoir was measured by means of three chromel-alumel thermocouples of the type used on the collector. The relative accuracy of the reservoir temperatures was estimated to be ±5°C. The absolute accuracy of the true reservoir temperature (i.e., the surface temperature of the liquid) depended on the level of the liquid in the reservoir. Considering the uncertainty in that level the absolute accuracy was estimated to be ±15°C.

12. Output current was measured at the cell instrumentation panel by means of a calibrated shunt. The accuracy was estimated to be ± 2 amps. Output lead voltage was measured by means of two sets of voltage probes (for redundancy) between the collector and emitter transition part. These probes were either of the same material as the parts being probed or of materials with similar thermoelectric characteristics to minimize errors. Measurement errors were ±0.02 volts. Output electrode voltages were not measured but were calculated on the basis of emitter stem resistance and the lead voltage.

13. Output current was measured at the cell instrumentation panel by means of a calibrated shunt. The accuracy was estimated to be ± 2 amps. Output lead voltage was measured by means of two sets of voltage probes (for redundancy) between the collector and emitter transition part. These probes were either of the same material as the parts being probed or of materials with similar thermoelectric characteristics to minimize errors. Measurement errors were ±0.02 volts. Output electrode voltages were determined using the collector probe for one and the positive leg of an intrafuel-clad thermocouple for the other. An accuracy of ±0.05 volts was estimated. In some cases the emitter electrode probe had become unreliable in which case the electrode voltage was calculated on the basis of measured emitter stem resistance and the lead voltage.

14. Not measured.

15. Measurement of relative values of the emitter work function were completed. These values were used in conjunction with performance data to estimate the emitter temperature as described in the body of this report.

16. Flowing helium boiled from liquid helium was the test environment. Gas chromatography of containment gas was performed. The sensitivity limit was on the order of 1 ppm.

17. Flowing helium boiled from liquid helium was the test environment. An oxygen analyzer with 0.1 ppm sensitivity was used to measure the oxygen content of the helium containment gas.

18. Helium boiled from liquid helium was the test environment. The containment was sealed and could not be sampled.

19. Argon (assay of impurities: $H_2 < 2$ ppm; $O_2 < 2$ ppm; $N_2 < 5$ ppm; $CH_4 < 2$ ppm; $CO < 3$ ppm; $CO_2 < 1$ ppm; $H_2O = 4$ ppm) was the test environment. These were sealed containments.

20. Same as 9 except only three thermocouples were used in collector.

21. Same as 9 except that only two thermocouples were used in collector.

22. Same as 10 except that lower skirt thermocouple was tied on in area of final closure braze.

APPENDIX B

DIAGNOSTIC PROCEDURE FOR DETERMINING EMITTER TEMPERATURES, RELATIVE POWER AND RELATIVE EFFICIENCY OF THERMIONIC CONVERTERS IN THE ABSENCE OF EMITTER THERMOCOUPLES

by

J. W. Holland
(GA-7298)

ABSTRACT

A method is presented for the determination of time-dependent emitter temperatures, output power, and efficiencies relative to initial values. The determinations are made by means of a correlation that relates changes in converter voltage caused by alteration of work functions to differences in plasma losses arising from cesium pressure changes required to maintain maximum converter voltage. Relative fission powers required for the calculation of the efficiency are determined by means of calorimetry of the thermal energy to the collector and the application of an energy balance. The calculational method is verified in experiments where emitter thermocouples were used.

INTRODUCTION

The determination of emitter temperature in fission heated thermionic converters both initially and over long duration tests is necessary for the evaluation of power density trends. Direct measurement of the emitter temperature by means of high temperature thermocouples is difficult because they must be placed into a thin wall emitter which is also the fuel cladding, and also, their reliability and stability for thousands of hours in the reactor environment has not been good. In addition, the presence of the emitter thermocouples has in some cases been suspected of reducing the reliability of the converter itself. For these reasons thermocouples were not used in many of the General Atomic past in-pile converter operations and there existed a need for some other method for the evaluation of performance.

In this analysis, emitter temperatures and output powers relative to initial values are computed by means of a correlation that relates changes in converter voltage to differences in plasma losses arising from cesium pressure changes required to maintain maximum cell voltage. Relative fission powers are calculated by an energy balance on the collector. The overall converter efficiency relative to the initial value is determined by combining the relative power calculation with the relative fission power determination.

PLASMA LOSS-CELL VOLTAGE CORRELATION

When voltage changes are observed at a given emitter and collector temperature and cell current they are accompanied by changes in optimum cesium reservoir temperatures.[1] The physics of these changes is explained in terms of altered electrode work functions which require different optimum cesium pressures to give the necessary optimum cesium coverage on the electrode surfaces. It has been shown that increased cesium pressure increases the plasma loss V_d[2] for values of the pressure-spacing product greater than 20 mil-torr, as demonstrated in the Kitrilakis[2] correlation curve shown in Figure 1.

According to the above arguments, changes in cell voltage dV due to work function alteration should be equal and opposite to changes in the plasma loss dV_d, expressed as

$$dV = -dV_d, \tag{1}$$

and changes in cell voltage should be calculable from changes in the optimum cesium reservoir temperature.

Calculated changes in cell voltage ΔV_{calc} may be directly obtained from Figure 2, which is a replot of Figure 1, where V_d is shown as a function of cesium reservoir temperature at a constant interelectrode spacing. Values of ΔV_{calc} computed from the data of reference 1 are shown in Figure 3 versus the observed voltage changes $\Delta V_{obs.}$ The 45° inclination of the line in Figure 3 substantiates the assumption of equation (1).

Figure 2 shows that from the slope of the V_d versus T_{Ropt} curve

$$dT_{Ropt} = 165\ dV_d \qquad 335 < T_{Ropt} < 390^\circ C. \tag{2}$$

It is noted that the linearization of the V_d curve according to equation (2) introduces an error less than 0.01 volt in V_d over the indicated limits, which will be seen to more than cover the range of interest. By combining equations (1) and (2), changes in T_{Ropt} are related to cell voltage changes due to work function alteration by the equation

$$dT_{Ropt} = -165\ dV, \tag{3}$$

which, as will be seen, forms the basis for the determinations of emitter temperatures and relative performance at times other than initially.

DERIVATION OF THE EMITTER TEMPERATURE EQUATION

Changes in the optimum cesium reservoir temperatures are caused not only by work function changes, but also by changes in cell current density, dJ, and by changes in emitter temperature, dT_E. Changes in collector

temperature near the optimum have not been observed to significantly alter T_{Ropt}. Changes in T_{Ropt} may be related to changes in the operating variables by the partial differential equation.

$$dT_{Ropt} = \left(\frac{\delta T_{Ropt}}{\delta T_E}\right) dT_E + \left(\frac{\delta T_{Ropt}}{\delta J}\right) dJ + \left(\frac{\delta T_{Ropt}}{\delta V_d}\right) dV_d. \qquad (4)$$

Values for the T_E and J coefficients in equation (4) have been experimentally determined from the out-of-pile test data shown in Figures 4 and 5. From Figure 4:

$$\left(\frac{\delta T_{Ropt}}{\delta T_E}\right) = 0.18^\circ C/^\circ C \qquad 1600 < T_E < 2000^\circ C. \qquad (5)$$

From Figure 5:

$$\left(\frac{\delta T_{Ropt}}{\delta J}\right) = 2.1^\circ C/amp/cm^2 \qquad 8 < J < 20 \text{ amp/cm}^2. \qquad (6)$$

Both equations (5) and (6) give values for the coefficients with less than $2^\circ C$ variation in T_{Ropt} from the curves displayed in Figures 4 and 5.

Substitution of equations (1), (2), (5), and (6) into equation (4) yields:

$$dT_{Ropt} = 0.18\ dT_E + 2.1\ dJ - 165\ dV. \qquad (7)$$

Each of the differential terms in equation (7) may be integrated from the initial operating time to a time t, for example,

$$\int_o^t dT_{Ropt} = (T_{Ropt})_t - (T_{Ropt})_o = \Delta T_{Ropt}. \qquad (8)$$

Integrations similar to equation (8) transform equation (7) into the difference equation:

$$\Delta T_{Ropt} = 0.18\ \Delta T_E + 2.1\ \Delta J - 165\ \Delta V. \qquad (9)$$

It is noted that ΔT_{Ropt} and ΔJ are measured quantities in the in-pile test, but ΔT_E and ΔV remain unknown; ΔV is unknown since it depends on ΔT_E. By writing ΔV as a function of ΔT_E, a second equation will be determined which allows simultaneous solution of both ΔV and ΔT_E.

To determine ΔV correctly, both V_t and V_o must be at equal emitter temperatures, collector temperatures, and currents, and the cesium reservoir pressure must be optimized for maximum voltage. Thus, either V_o must be corrected to the conditions at time t, or V_t must be corrected to the initial conditions. The same result is obtained either way. The former choice is selected since the initial performance characteristics are available in the performance maps of the Mark VI out-of-pile converter OC-5, which are used in the calculations. On the basis selected,

$$\Delta V = \left[V_t(T_{Et}) - V_o(T_{Et})\right]_{J_t,\ T_{Ct}} \tag{10}$$

For a given cell current J_t, an equation for $V_o(T_{Et})$ may be written for each of current curves shown in Figure 6 as a linear function of emitter temperature in the form

$$\left[V_o(T_{Et})\right]_{J_t,\ T_{Ct}} = \left[a\ T_{Et} - b\right]_{J_t,\ T_{Ct}} \tag{11}$$

If the collector temperature T_{Ct} varies from the 700° C value for which the performance map of Figure 6 was made, then an added correction must be made for b which, in effect, vertically shifts the constant current curves to lower voltages. The amount of the voltage shift Δb is shown in Figure 7 as a function of T_C, which is expressed as

$$\Delta b = b\ (T_{Ct}) - b\ (T_C = 700^\circ C). \tag{12}$$

This correction is strictly valid only at $T_E = 1800^\circ$ C, but the inaccuracy admitted by using the correction at $1600 < T_E < 1900$ is insignificant. Equation (10) may be rewritten, substituting equation (11) and including Δb, as

$$\Delta V\ (T_{Et},\ T_{Ct})_{J_t} = V_t - a\ T_{Et} + b + \Delta b. \tag{13}$$

Equation (13) forms the second equation that is required for a solution of T_{Et}. Substitution of equation (13) into equation (9) and solving for T_{Et} gives

$$T_{Et} = \frac{\Delta T_{Ropt} + 0.18\ T_{Eo} + 165\ (V_t + b + \Delta b) - 2.1\ \Delta J}{0.18 + 165a} . \qquad (14)$$

Values of T_{Et} derived by means of this equation are used to calculate the relative power and efficiency of IC-6 through IC-12 at various times in their operation. The validity of the computation method for determining the emitter temperature by means of equation (14) is experimentally verified in the section of Experimental Verification of Analytical Method for Determining T_E and P_r. The constants used in equation (14) are, of course, valid only for the particular type of converter for which they were derived.

RELATIVE POWER DENSITY

The power density at time t relative to initial conditions is defined as

$$P_r = \left(\frac{P_t}{P_o}\right)_{T_{Et},T_{Ct},J_t,T_{Ropt}} \qquad (15)$$

For a valid comparison, the initial and time t power densities must be at equal conditions. Since it is a rare occurrence that both the initial and time t powers are at equal emitter temperatures, collector temperatures, and cell currents in a reactor test, either P_t or P_o must be corrected to the conditions of the other. It has been elected to correct the initial power density to the conditions at time t as indicated by equation (15). Since the currents are equal in the definition, equation (15) can be written in terms of voltages, or

$$P_r = \left(\frac{V_t}{V_o}\right)_{T_{Et},T_{Ct},J_t,T_{Ropt}} \qquad (16)$$

Employing T_{Et} as previously determined by equation (14), it is convenient to find

$$(V_o)_{T_{Et},T_{Ct},J_t}$$

from the performance map of Figure 6, and make the correction to the voltages due to a deviation of the collector temperature from 700° C. The quantity

$$(V_t)_{T_{Et},T_{Ct},J_t}$$

is, of course, the measured value of cell voltage; thus, the relative power is readily computed by means of equation (16). Deviations from unity by the relative power would be caused by work function changes, assuming there were no alterations in the interelectrode gap or in the scattering of electrons by a foreign gas. Computed values of P_r are compared to measured values in the section on Experimental Verification of Analytical Method for Determining T_E and P_r.

Relative Efficiency

The efficiency at time t relative to the initial efficiency is defined by

$$\eta_r = \left(\frac{\eta_t}{\eta_o}\right)_{T_{Et},T_{Ct},J_t,T_{Ropt}} = \left(\frac{P_t}{Q_t} \cdot \frac{Q_o}{P_o}\right)_{T_{Et},T_{Ct},J_t,T_{Ropt}} = \left(P_r \cdot \frac{Q_o}{Q_t}\right)_{T_{Et},T_{Ct},J_t,T_{Ropt}} \qquad (17)$$

where Q_o and Q_t are the total fission power inputs initially and at time t, and P_r is determined by equation (16). Values for Q_o are determined from the out-of-pile converter OC-5 data, an example of which is shown in Figure 8. These data, in the form of T_E versus Q, are assumed to represent the initial energy transfer condition of the in-pile coverter operating under optimum conditions, since both the in-pile converters and OC-5 employed the same materials and geometry. Corrections due to small col-

lector temperature variations are neglected since their effect on input power is negligible.

The quantity Q_t is determined by the expression

$$Q_t(T_{Et},T_{Ct},J_t,T_{Rt}) = Q_o(T_{Eo},T_{Co},J_o,T_{Ro}) + \Delta Q \tag{18}$$

The quantity ΔQ is derived in the following sequence. By considering a balance of energy, it can be stated that the total fission and gamma heat Q generated within the fuel and emitter is transformed into electrical energy P and is dissipated as waste heat Q_C arriving at the collector and thermal losses Q_{EL} from the emitter structure, or

$$Q = P + Q_C + Q_{EL} \tag{19}$$

Heat leaving the collector structure, Q_{CL}, is born from three sources: the emitter-to-collector waste heat Q_C, gamma heating $Q_{C\gamma}$ in the collector structure, and collector heater power Q_{CH}. It is expressed as

$$Q_{CL} = Q_C + Q_{C\gamma} + Q_{CH} \tag{20}$$

Solving equation (20) for Q_C and substituting into equation (19) yields

$$Q = Q_{CL} - Q_{C\gamma} - Q_{CH} + P + Q_{EL} \tag{21}$$

Equation (21) may be rewritten as an equation of finite differences, where ΔQ or ΔP is defined as the power at any time minus the power at the beginning of the operation, or

$$\Delta Q = \Delta Q_{CL} - \Delta Q_{C\gamma} - \Delta Q_{CH} + \Delta P + \Delta Q_{EL}. \tag{22}$$

For small changes in emitter temperature, ΔQ_{EL} is a second-order term and is assumed negligible. All of the remaining terms on the right of equation (22) are experimentally determinable, and thus their summation provides a value for changes in fuel fission power. The only term on the right of equation (22) that has any relation to a reactor variable is the collector

gamma heating terms, $Q_{C\gamma}$ but this term has been shown to be of low magnitude compared with the total input power in TRIGA tests and has been neglected.

Values for ΔQ_{CH} and ΔP are directly measured by means of the converter instrumentation. A calorimetric method for the determination of ΔQ_{CL} was developed which allowed calculation of ΔQ_{CL} from changes in collector temperature ΔT_C. Collector heat is transferred to the reactor water across a helium gap and since the reactor water remains at nearly a constant temperature, it is predicted that ΔQ_{CL} would be directly proportional to ΔT_C, related by a proportionality constant, U, or

$$\Delta Q_{CL} = U\Delta T_C. \tag{23}$$

Values of U were determined for each test by means of the collector heater, so that U could be found as a function of T_C by

$$U = \frac{\Delta Q_{CH}}{\Delta T_C}, \tag{24}$$

where during the calibration $\Delta Q_C = \Delta Q_{C\gamma} = 0$. Values of ΔQ_{CL} are estimated to be within ± 20% correct by this calorimetric method.

Equation (22) is rewritten in terms of the aforementioned stipulations as

$$\Delta Q = U\Delta T_C - \Delta Q_{C\gamma} - \Delta Q_{CH} + \Delta P. \tag{25}$$

Substitution of equation (25) into equation (18) gives the input power at t relationship that is required for solution of the relative efficiency, or

$$Q_t(T_{Et},T_{Ct},J_t,T_{Rt}) = Q_o(T_{Eo},T_{Co},J_o,T_{Ro}) + U\Delta T_C - \Delta Q_{C\gamma} - \Delta Q_{CH} + \Delta P. \tag{26}$$

Deviations in the relative efficiency from unit arise from the combined effects of power output changes and changes in heat transfer such as would result from electrode emittance change, from the introduction of a thermally conducting gas or from a change in electron waste heat.

Experimental Verification of Analytical Method for Determining T_E and P_r

The electrically heated life test converter LC-5 was tested with emitter thermocouples and, therefore, provided an excellent test of the accuracy of the T_E and P_r computation methods described in the preceding sections. Converter LC-5 had another advantage in that its initial performance was equal to that expected from a converter with an emitter work function of 4.6 ev, which was also characteristic of the in-pile converters for which the method is intended. The data to be compared was obtained during time of high confidence in the emitter temperature determinations. Values of T_E computed by equation (14) and of P_r by equation (16) are compared to the measured values in Table 1, where there is observed a very close comparison. The maximum difference between the calculated and measured emitter temperature is shown to be 12° C or 0.5%, while the maximum deviation between the calculated and measured relative powers is 3%.

Table 1

COMPARISON OF MEASURED EMITTER TEMPERATURE AND RELATIVE POWER WITH COMPUTED VALUES BY ANALYTICAL METHOD FOR NASA LIFE TEST CONVERTER LC-5

Operation Time (Hr.)	Emitter Temp. T_E (° C)		Relative Power P_r	
	Meas.	Calc.	Meas.	Calc.
0	1748	1748	1.00	1.00
22	1747	1752	0.97	0.99
139	1747	1744	0.95	0.98
1081	1750	1742	0.93	0.94
3287	1759	1767	0.87	0.86
7162	1737	1749	0.88	0.87

REFERENCES

1. Holland, J. W., "Final Report on Thermionic Conversion Programs," Bureau of Ships Report, GA-6572, General Atomic Division, General Dynamics Corp., August 25, 1965. (U)

2. Kitrilakis, S. S., A. Shavit, and N. S. Rasor, "The Department of the Observed Performance from the Idealized Case in Cesium Thermionic Converters," in Report on Twenty-Fourth Annual Conference on Physical Electronics, March 25, 26, and 27, 1964, Massachusetts Institute of Technology, Cambridge, Massachusetts, pp. 171-184. (U)

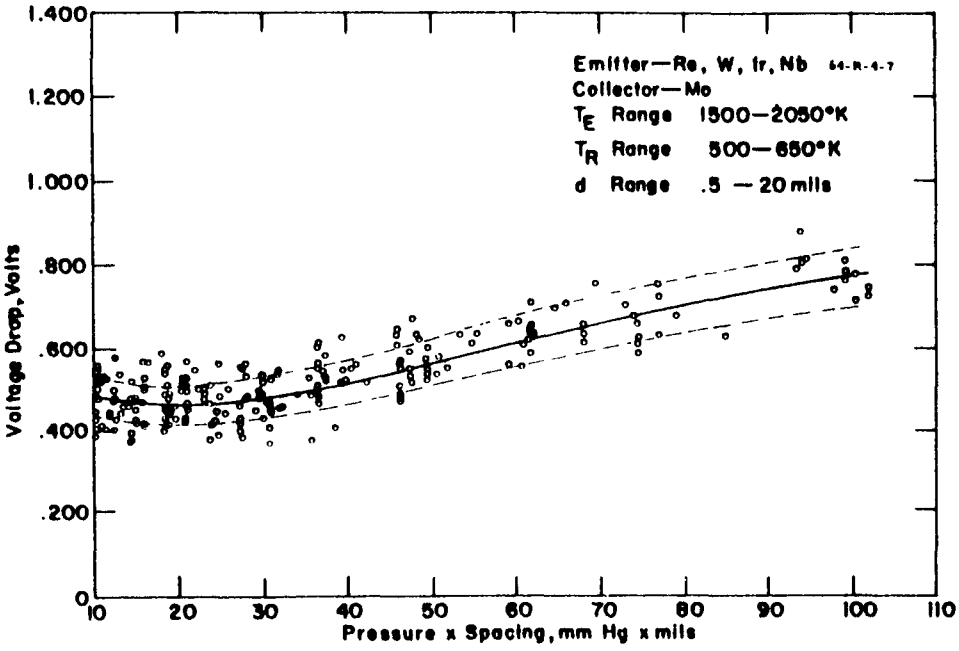

FIGURE 1. VOLTAGE DROP AS A FUNCTION OF PRESSURE-SPACING PRODUCT (FROM REFERENCE 2)

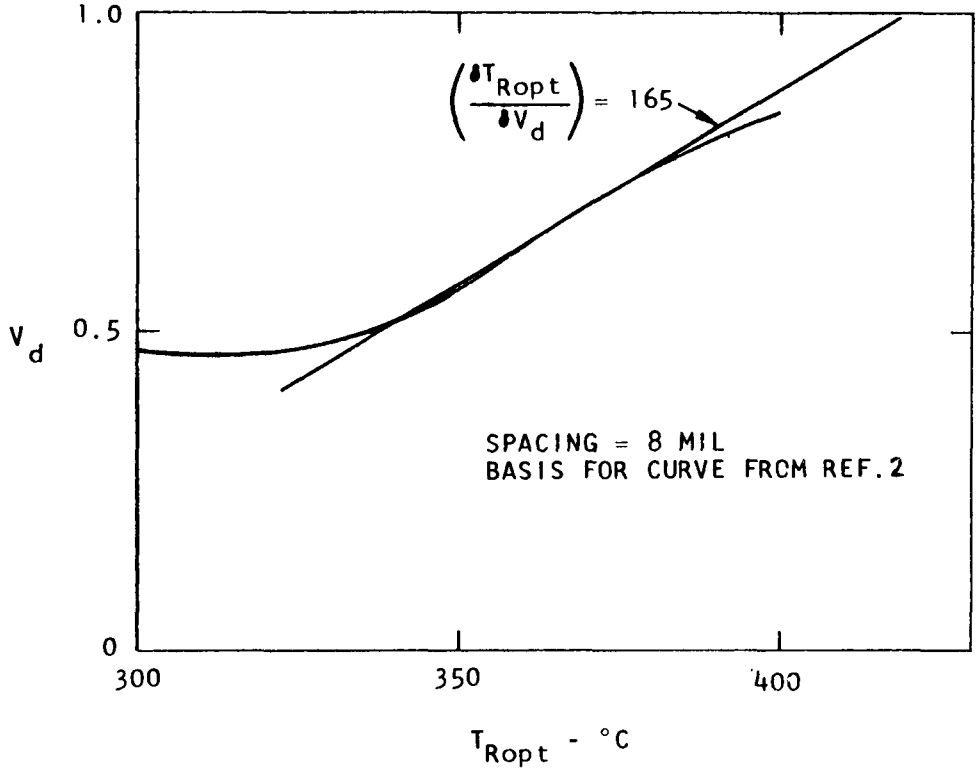

FIGURE 2. PLASMA LOSS V_d VERSUS OPTIMUM CESIUM RESERVOIR TEMPERATURE.

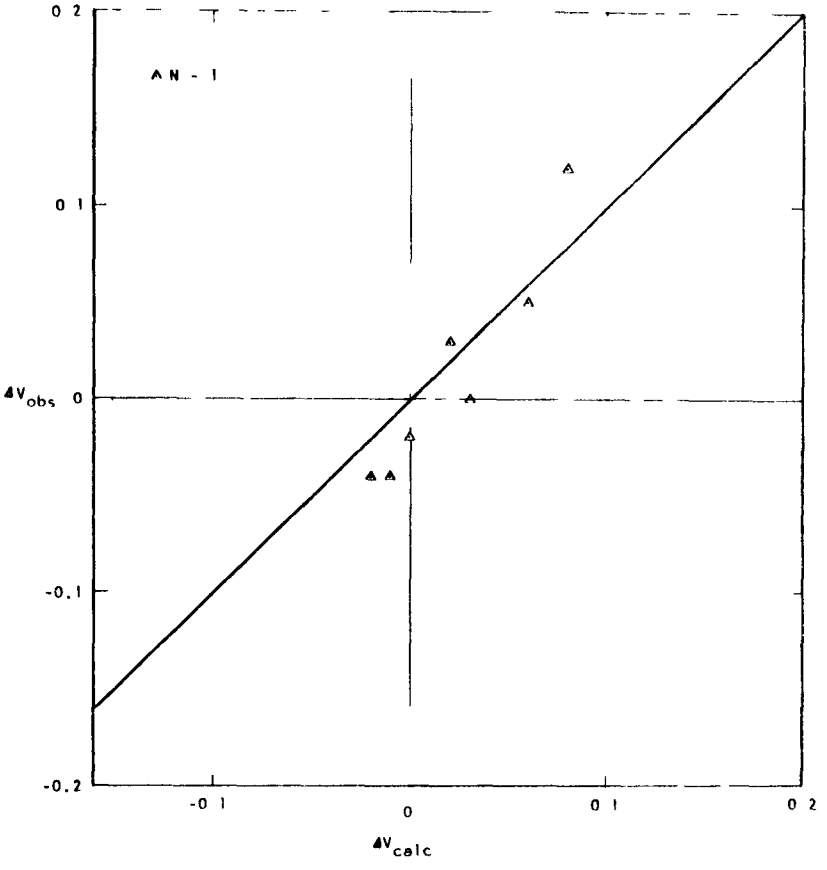

FIGURE 3. CORRELATION OF CALCULATED AND OBSERVED VOLTAGE LOSSES.

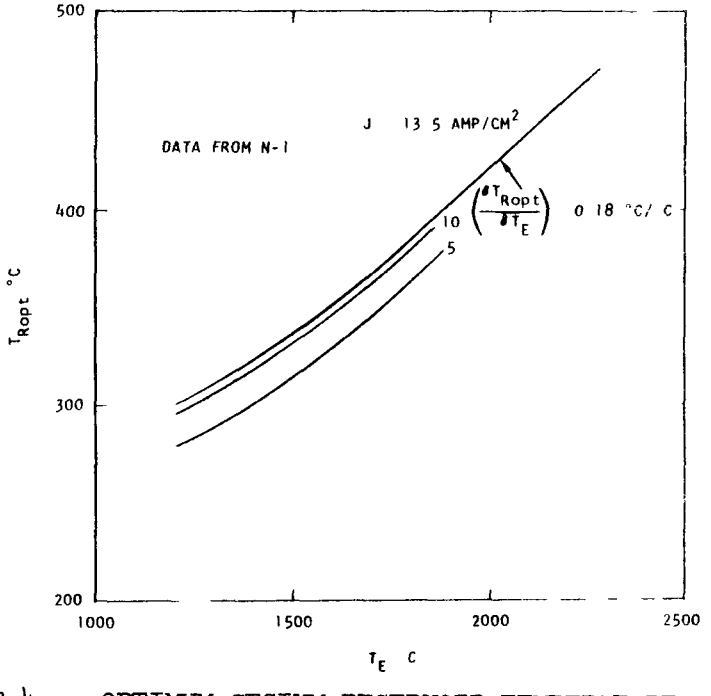

FIGURE 4. OPTIMUM CESIUM RESERVOIR TEMPERATURE VERSUS EMITTER TEMPERATURE.

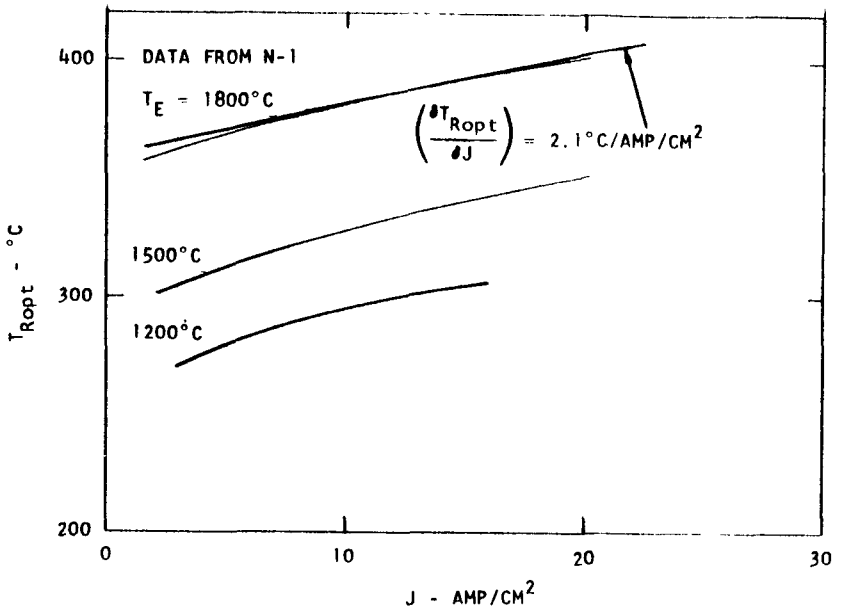

FIGURE 5. OPTIMUM CESIUM RESERVOIR TEMPERATURE VERSUS CELL CURRENT DENSITY.

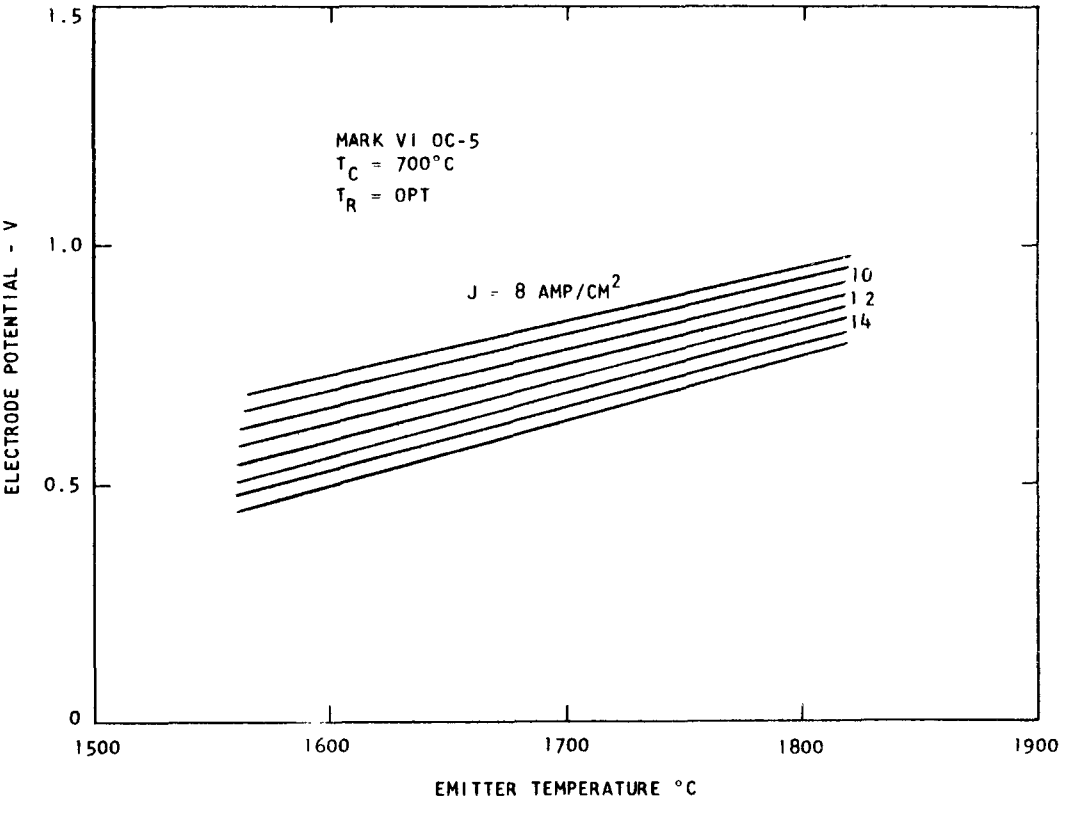

FIGURE 6. ELECTRODE POTENTIAL VERSUS EMITTER TEMPERATURE OF MARK VI OC-5.

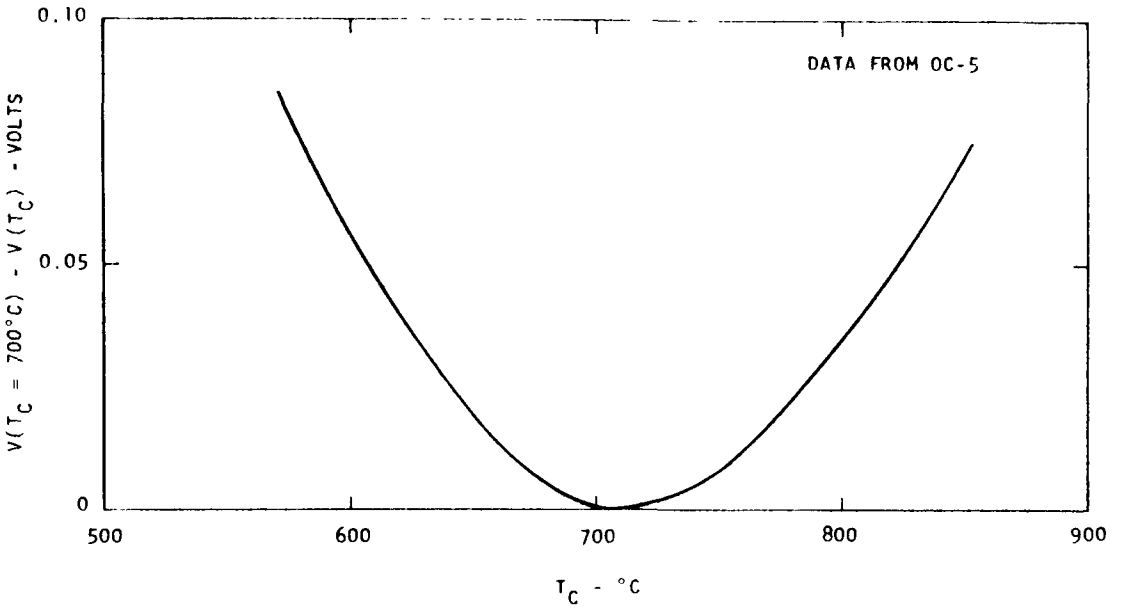

FIGURE 7. VOLTAGE CORRECTION FOR DEVIATIONS OF COLLECTOR TEMPERATURE FROM OPTIMUM AND Δb.

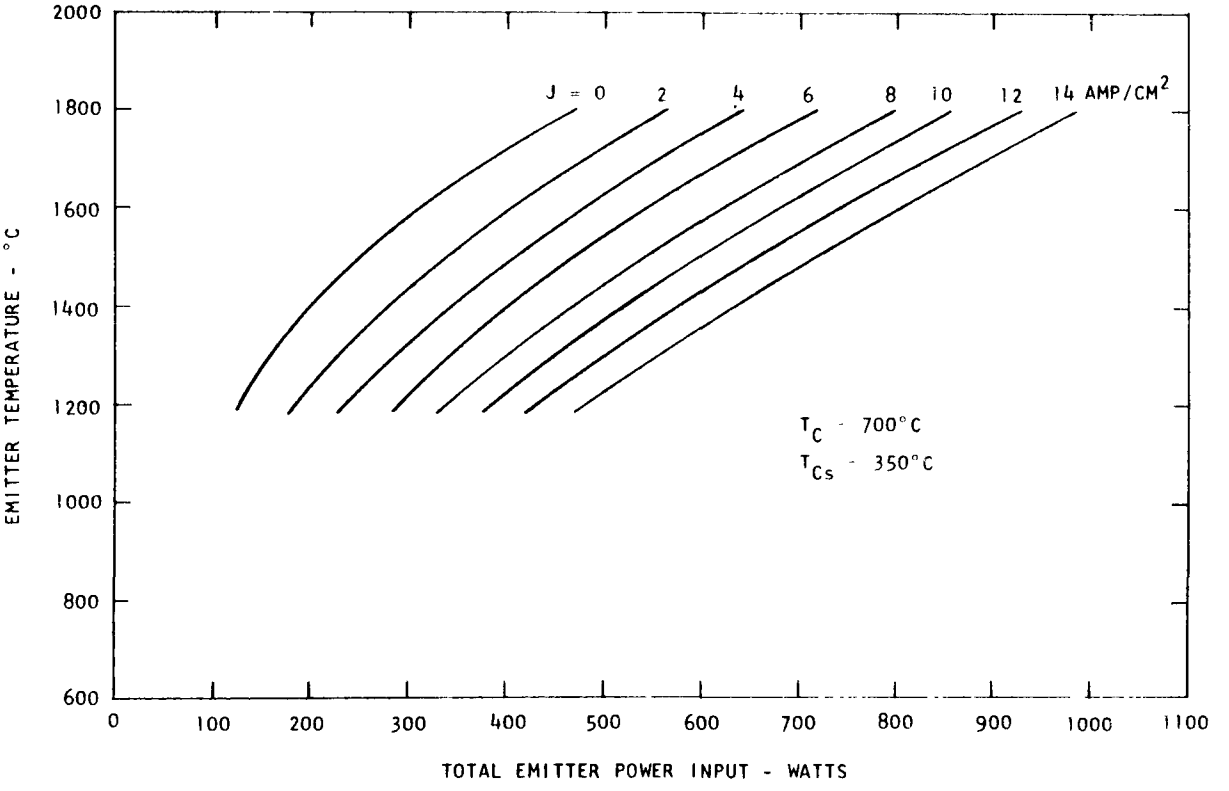

FIGURE 8. MARK VI OC-5 EMITTER TEMPERATURE VERSUS INPUT POWER, WITH CURRENT DENSITY SHOWN AS A PARAMETER.